A PHOTOGRAPHIC EMULSION STUDY OF THE NUCLEAR PHOTODISINTEGRATION OF HELIUM

A Thesis Presented by

IAIN GRANT MAIN, B.Sc., M.A.

in Application for the Degree of

Doctor of Philosophy

UNIVERSITY OF ST ANDREWS

1960

DECLARATION

I declare that this thesis has been composed by me, that the work of which it is a record has been done by me, and that it has not been accepted in any previous application for a Higher Degree.

STATEMENT OF RESEARCH TRAINING

Having studied for four years in St Salvator's College, I graduated B.Sc. with First Class Honours in Natural Philosophy in 1955.

After one year's higher study and research as Shell Oil Fellow in Queen's University at Kingston, Ontario, I was awarded that University's degree of M.A. in Physics, for a thesis entitled "Energy and Angular Distributions of Photo-protons from Indium".

I was awarded a Research Studentship in Nuclear Physics by the University of Glasgow, where I spent the academic year 1956-57.

In 1957 I was appointed Lecturer in Physics in Queen's College, and have pursued research work in conjunction with my teaching duties. I was admitted as a part-time Research Student under Ordinances Nos. 16 and 61 on 1st January 1958, since when I have completed the equivalent of six terms of full-time research under the supervision of Professor G. D. Preston. I submit the accompanying thesis at this time with the approval of the Senatus Academicus under Section III(2) of Ordinance No. 61.

30th September 1960

CERTIFICATE

I certify that Iain Grant Main, B.Sc., M.A. has spent six terms at research work under my supervision in the Carnegie Laboratory of Physics of the University of St Andrews, and that he has fulfilled the conditions of Ordinances Nos. 16 and 61 and the accompanying Regulations of the Senatus Academicus.

Research Supervisor

CONTENTS

(P.T.O.)

CONTENTS (CONTINUED)

ABSTRACT

Photodisintegration of the α-particle has been studied by examining photographic plates, previously exposed to ionizing radiation resulting from the bombardment of helium by high-energy X-rays.

Relevant theory is surveyed briefly, and a review is made of previous experimental work on the subject. The results of the investigation are presented after a description of the experimental technique, measurements and analysis.

From an exposure in which the maximum X-ray energy was nominally 35 MeV, the shape of the broad resonance in the (γ,p) cross section has been determined, and is compared with previous measurements. Angular distributions reveal a larger percentage of electric quadrupole absorption of photons than previously ascribed to the reaction, but show no evidence of any magnetic dipole absorption.

An exposure at 70 MeV has been used to demonstrate

that the (γ,p) and (γ,n) cross sections are similar at photon energies above the resonance. The photoneutron angular distribution is asymmetric, and cannot be explained by any existing theory.

No evidence has been found that multiple processes occur with frequency comparable with (γ,p) and (γ,n).

1 INTRODUCTION

1: INTRODUCTION

Chadwick and Goldhaber (1934) were the first workers to detect the disintegration of a nuclear structure by electromagnetic radiation, when they succeeded in breaking the deuteron into its constituent neutron and proton under irradiation with 2.62-MeV γ-rays from ThC". Encouraging theoretical agreement followed from Bethe and Peierls (1935), and deuteron photodisintegration has since been very thoroughly investigated both experimentally and theoretically, and some hundreds of papers published on the subject.

The degree of understanding reached in the case of the two-nucleon system has not so far been achieved for other nuclei. Szilard and Chalmers (1934) initiated the study of more complex nuclei by detecting photoneutrons from beryllium; for fairly light nuclei, it is possible to study individual nuclear levels and transitions, and selection rules consequent upon the charge independence of nuclear

forces sometimes simplify the interpretation of results in these cases. Resonance effects are common in the absorption of γ-rays by light nuclei, since the energy states in the excited nucleus have widths much smaller than their distance apart.

For nuclei with atomic numbers greater than about 20, overlapping of energy levels occurs, with the result that their individual effects are not observed. For a given photon energy, many levels will contribute to a photonuclear cross section, and its study is divided into two stages. These stages--the mechanism of photon absorption by the nucleus, and the subsequent emission of particles--can be clearly separated when the excitation energy is low enough for the "compound nucleus" picture of N. Bohr (1936) to be a reliable one, i.e. up to about 50 MeV. "Direct" effects must be expected at higher excitation energies. In any case, the mathematical complexity at present surrounding the nuclear many-body problem dictates that any theoretical approach be a phenomenological one, in the hope that a satisfactory nuclear model, if found, can ultimately help to elucidate the basic interactions involved.

The experimental methods of studying the photo-disintegration process are largely dependent on the γ-ray

sources available. Natural radioactive substances are of poor intensity for studying effects whose cross sections are measured only in millibarns, and are severely restricted in energy. Radiative particle capture, notably in the reaction $Li^7(p,\gamma)Be^8$, provides more intense sources of radiation with energies up to about 20 MeV available; by accelerating the charged particles to a common resonance energy, the radiation can be made strictly monochromatic, but is restricted to a few fixed energies. Miller et al. (1960) have recently suggested a means of providing monochromatic γ-rays of continuously variable energy from the annihilation in flight of positrons.

The absence of a single, well-defined γ-ray energy is the principal drawback inherent in the use of an electron accelerator--linear accelerator, betatron or synchrotron--which is the only available source of radiation of very high energy. The output of such a machine is a continuous spectrum of bremsstrahlung X-rays having all energies from zero up to the energy to which the electrons are accelerated, and the "difference" methods (e.g. Katz and Cameron 1951, Penfold and Leiss 1959) which have to be used to derive a reaction cross section from a yield curve are of poor resolution. Nevertheless the form of the excitation function has been derived for a large number of nuclei and reactions. The

characteristic shape is a broad, smooth peak known as the "giant resonance", the systematics of whose parameters--width, peak height, resonance energy, etc.--are valuable experimental data. Detailed investigation of the emitted particles is also valuable; their angular distribution helps to identify the character of the photon absorption, and their energy spectrum can be compared with that expected when particles are "evaporated" from an excited nucleus or ejected in some kind of direct interaction with the photon. Deviations from a statistical model have been indicated by measurements of the branching ratios between different induced reactions.

The photon absorption is less easy to study experimentally than the particle emission stage of a reaction. Investigation must proceed indirectly, since the nuclear cross sections are so very much smaller than those for the various electronic forms of absorption. It is necessary to measure the partial cross section curves for each of the several reactions of a given nucleus (where possible) and construct the curve of absorption cross section against photon energy from these.

The present study concerns the α-particle, the simplest structure readily available for experiment, next to the deuteron. As will be shown in succeeding sections, no successful detailed treatment has so far been given for this

nucleus, although some agreement with experimental results has been achieved at a few points. He^4 is experimentally attractive since it is light enough for neither of the product particles in any two-body disintegration to have any excited energy states, with the result that the photon absorption is more directly accessible to measurement. The excitation function for any such reaction can be derived completely from measurements on either particle alone, even with a bremsstrahlung beam.

After the theoretical review, the present state of experimental knowledge of this nucleus will be assessed, by way of introduction to the description of the present study and the presentation and discussion of the experimental results.

2 REVIEW OF PHOTODISINTEGRATION THEORY, WITH SPECIAL REFERENCE TO THE ALPHA-PARTICLE

2: REVIEW OF PHOTODISINTEGRATION THEORY, WITH SPECIAL REFERENCE TO THE ALPHA-PARTICLE

2.1 The Multipole Classification

When dealing with nuclear reactions induced by particles it is customary to classify the particles in the incident beam according to "partial waves", to each of which corresponds a certain particle angular momentum. In a similar way, it is convenient to classify electromagnetic radiation according to the successive terms of a general expansion known as the multipole representation.

The quantum theory of radiation, using the classical representation of a radiative source (or absorber) as an oscillating electric or magnetic moment, leads to the expression of the radiation in terms of a convergent series of powers of $(R/\lambda\!\!\!^{-})$, where R is the radius of the charge-current system and $\lambda\!\!\!^{-}$ is $(1/2\pi)$ times the wavelength of the radiation. The classical condition $(R/\lambda\!\!\!^{-}) \ll 1$ limits the number of

appreciable terms in the expansion; these will be few for nuclei and γ-rays up to quite high energies, since $\lambda\!\!\!^{-}$ (although inversely proportional to the energy) has the value 197×10^{-13} cm at 1 MeV.

The angular momentum of a photon with respect to the absorbing nucleus is determined by quantum numbers l and m similar to those for a particle. Angular momentum is conserved in the photon-nucleus system, so that $l = |\vec{J}_f - \vec{J}_i|$, where $\vec{J}_i$ and $\vec{J}_f$ are the (vector) angular momenta of the initial and final nuclear levels. Thus l can have any value given by

$$|J_f - J_i| \leqslant l \leqslant (J_i + J_f)$$

except the value zero, excluded as a consequence of the transverse nature of electromagnetic radiation. The value 2^l is called the multipole order of the radiation.

There are two independent partial waves for each value of l, the one actually obtained depending on whether or not a change of the parity of the nucleus occurs in the transition. The multipole having the same parity as a particle with the same l, i.e. $(-1)^l$, is termed an electric multipole; the multipole with parity $-(-1)^l$ is called magnetic. These are usually designated by the respective symbols E and M, followed by the value of l.

The probability of transition from a nuclear state ψ_i to state ψ_f is proportional to the absolute square of the "matrix element", given by the integral

$$M_{if} = \int \psi_i q \psi_f \, d\tau$$

where $d\tau$ is a volume element and q is the effective electric or magnetic moment. Even if we can estimate the various multipole moments present in the nucleus, it is not possible to calculate M_{if} explicitly without detailed knowledge of the wave functions ψ_i and ψ_f. But knowledge of their parity alone indicates which transitions are forbidden (i.e. have zero probability) and leads to the enumeration of selection rules. For example, for electric dipole radiation q has the form $\sum e_i x_i$, and will change sign on reflection in the origin of coordinates. Thus ψ_i and ψ_f must have opposite parity if the matrix element (a definite integral) is not to change sign also, necessitating the value zero. Conservation of parity in the whole system means that in electric dipole radiation the photon must have odd parity with respect to the nucleus. Similar considerations for other multipoles lead to the selection fules, summarized in the statement:

"For an El (Ml) transition, the parity of the nucleus changes unless l is even (odd)".

Quantitative estimates of transition probabilities must depend on the nuclear model adopted for the calculation. However, a general result is that the probability of radiation decreases roughly as $(R/\lambda\!\!\!^{-})^{2l}$, so that the multipole observed is usually just that given by the smallest value of l consistent with angular momentum conservation. Moreover, the intensity of magnetic 2^l-pole radiation is considerably less than that of the corresponding electric multipole. However, contrary to the situation in atomic spectroscopy, these reductions do not render the transitions other than E1 "forbidden". In nuclear processes relative intensities are much less important experimentally, since transition probabilities can be directly measured with greater accuracy; nuclei are not subject to external influences tending to remove them from long-lived states. In addition, such transitions in nuclei are not obscured by overlapping electric dipole transitions to the same extend as in atomic systems.

2.2 The Photodisintegration Process

As already stated, there are two extremes of behaviour which can be expected to lead to the emission of a particle from a nucleus which has absorbed a photon: a "compound nucleus" may be formed by the sharing of the available energy among the nucleons in the target nucleus, and a particle

subsequently emitted by a chance concentration of sufficient energy; alternatively, the absorption may be localized, resulting in the instantaneous emission of a particle or particles.

The compound nucleus picture of the reaction has been developed according to several nuclear models, used to derive explicit wave functions. Goldhaber and Teller (1948) suggested a number of semi-classical models for the electric dipole process in which the neutrons and protons are treated collectively. These models were successful in producing an excitation function consisting of a broad resonance, whose width was interpreted as a damping effect. Steinwedel and Jensen (1950) and Danos (1952) made more detailed calculations using the most successful of these hydrodynamical models, and Ferentz, Gell-Mann and Pines (1953) succeeded in producing similar results by more rigorous quantum-mechanical means. More recently, Danos (1958) and Okamoto (1958) have shown that the application of the model to deformed nuclei leads to a splitting of the dipole resonance, and have extended the treatment to include quadrupole effects.

On the assumption of compound nucleus formation, the energy distribution of the photonucleons emitted may be calculated statistically, taking into account the correct

binding energy for the particle in question and allowing for the inhibited penetration of the Coulomb barrier by protons. Experiments have shown that this is in fact the main process for heavy nuclei, but that it cannot be the only form of interaction. In particular, too many high-energy photoprotons are found.

The first detailed direct-interaction theory was that of Courant (1951), who used a simple model in which each nucleon moved independently under a square-well potential. Matrix elements were calculated between this state and a similar final unbound state. The results were broadly similar to those of experiments on photoprotons from heavy elements, but detailed agreement was lacking.

Wilkinson (1956 and 1959) has shown how the independent particle model can be used to describe the features of the giant resonance. In this case, the outer "valence" nucleons alone cannot explain the resonance, since its integral with respect to quantum energy is given by a sum rule involving all the nucleons (See section 2.4). When absorption by transitions from closed shells of the nuclear core is considered, it transpires that relatively few of these are important, and that these few are of sufficient strength to account for most of the electric dipole sum.

Further, these transitions cluster together in such a way as to give a resonant shape to the absorption. To produce the correct absolute resonance energy, it is necessary to use a velocity-dependent potential such that the effective nucleon mass is about one-half of the free mass (Rand 1957). It is not yet clear whether such discrepancies as do exist with experimental resonance shapes disappear with the introduction of refinements, or whether some more fundamental modification will be required.

It is thought that the collective and independent particle pictures are not as irreconcilable as may at first appear; in any case, a compound nucleus may be formed by the sharing of the energy of an excited nucleon before it is emitted. The photonucleon energy distribution can be predicted by Wilkinson's theory, and the yield of high-energy protons agrees more closely with experiment than does the simpler theory of Courant.

Brief mention should be made of the possibility of photon absorption by a nuclear subunit of several nucleons. Such a process is logically intermediate between collective and single-particle absorption. Levinger (1951) has proposed the "pseudo-deuteron" model for photodisintegration at high γ-ray energies, where the wavelength is so small that only

occasionally will it encompass two nucleons. If a neutron and a proton come close together, the photodisintegration of the system will be similar to that of a free deuteron, modified by the momentum distribution of the particles inside the nucleus. At sufficiently high energies, each particle will take away half of the available energy. Dedrick (1955) has made numerical calculations of more detailed predictions of this model with which the results of experiments may be compared.

2.3 Cross Section Calculations for He^4

First-order perturbation theory gives the cross section for an electromagnetic transition from an initial state of a nucleus to a final state l as proportional to the sum $\sum_{m=-l}^{+l} |M_{if}|^2$ over all possible final spin states. As already explained, the calculation of the matrix elements M_{if} for the transitions from the ground state of He^4 to various unbound states will provide results which can be compared directly with experimental observations of photodisintegration cross sections; the main difficulty is lack of information on the correct forms of the wave functions to be used for the various nuclear ground states.

The most important type of photodisintegration

reaction in He^4 is the break-up into particles of masses 3 and 1, i.e. the processes $He^4(\gamma,p)H^3$ and $He^4(\gamma,n)He^3$. Since the He^4 nucleus contains equal numbers of protons and neutrons, these "mirror reactions" should be identical (apart from slightly different thresholds) in all respects unconnected with Coulomb forces.

It is convenient to use spectroscopic notation for the description of the various nuclear states involved. If we initially neglect terms other than $^1S_0$ in the ground state of the α-particle (Gerjuoy and Schwinger 1942), we can write down the transitions to all possible final interaction states and deduce the multipoles absorbed by means of the selection rules of section 2.1. Knowing that each of the product particles has intrinsic angular momentum $\frac{1}{2}$, we restrict ourselves to states in which these spins are antiparallel or parallel, i.e. singlet or triplet states. Considering only transitions involving dipole or quadrupole absorption, we draw up the list given in Table I. (The transitions $^1S_0 \rightarrow {}^1S_0$ and $^1S_0 \rightarrow {}^3P_0$ are forbidden, since the conservation law would require the radiation of zero angular momentum.)

If we further assume that the nuclei H^3 and He^3 are also in pure S-states (i.e. consider only central internucleon forces), we are left with transitions in which either

the multiplicities (for magnetic transitions) or the orbital angular momenta (for electric) change, but not both together.

Table I

Transitions from ground state of He^4 to (p + t) or (n + He^3)

$^1S_o \rightarrow {}^1P_1$	$\Delta J = 1$, yes[x]	E1
$^1S_o \rightarrow {}^1D_2$	$\Delta J = 2$, no	E2
$^1S_o \rightarrow {}^3S_1$	$\Delta J = 1$, no	M1
$^1S_o \rightarrow {}^3P_1$	$\Delta J = 1$, yes	E1
$^1S_o \rightarrow {}^3P_2$	$\Delta J = 2$, yes	M2
$^1S_o \rightarrow {}^3D_1$	$\Delta J = 1$, no	M1
$^1S_o \rightarrow {}^3D_2$	$\Delta J = 2$, no	E2

These are:

electric: $^1S_o \rightarrow {}^1P_1$, E1

$^1S_o \rightarrow {}^1D_2$, E2

magnetic: $^1S_o \rightarrow {}^3S_1$, M1

We can expect these transitions to be predominant, even if

[x] i.e. the parity changes.

some non-central forces are in fact present.

Flowers and Mandl (1951) adopted simple Gaussian spatial wave functions for the nuclei involved, and described the motion of the nucleons in the final state by plane waves. Making rough assumptions about inverse range parameters involved, they derived an expression for the cross section of the electric dipole process. The resulting function broadly resembled the giant resonances familiar in heavy nuclei; it rose rapidly to a broad maximum well above 30 MeV, and had a magnitude of the order of 1 millibarn. These authors also calculated the electric quadrupole cross section; the magnetic dipole cross section was not calculated explicitly, but was shown to be extremely small.

Gunn and Irving (1951) considered the electric dipole case only. They again neglected interaction between the product particles, but regarded Gaussian wave functions as unsatisfactory because of their poor asymptotic behaviour. They added calculations using exponential functions of a type previously introduced by Irving (1951) for variational calculations of binding energies. As they expected, these resulted in rather higher cross section values than the Gaussian functions, but again choice of values for the inverse ranges was to some extent arbitrary. Using figures which

gave correct values for the binding energy of He^4 and the Coulomb energy of He^3, they again found a broad peak in the excitation function, about 2 millibarns high and at a somewhat lower energy than the Flowers and Mandl result. Different choices of parameters resulted in fairly large changes in peak position and height.

Although these theoretical calculations gave cross section curves of the same general form as the experimental results then known, the closest fit was obtainable only by choosing an inverse range for He^4 which was very different from that required to give the correct binding energy. Bransden, Douglas and Robertson (1957) tried to remove the inconsistency by reducing the initial simplifications made by Gunn and Irving. After showing that the introduction of a final state interaction was no improvement on the plane wave representation of the outgoing nucleon, they repeated the calculation using tensor force wave functions (Irving 1953, Abraham, Cohen and Roberts 1955). This however was unsuccessful, and these authors (and Wilkinson 1959) have suggested the construction of new α-particle wave functions assuming a "hard core" two-body interaction potential.

The disintegration into two deuterons (spin 1) may be discussed in a similar fashion. Possible final states

(making allowance for the identity of the disintegration products) are:

$$^1S, ^1D, \ldots, ^3P, ^3F, \ldots, ^5S, ^5D, \ldots$$

Dipole and quadrupole transitions are given in Table II. On

Table II

Transitions from ground state of He^4 to (d + d)

$^1S_o \rightarrow ^1D_2$	$\Delta J = 2$, no	E2
$^1S_o \rightarrow ^3P_1$	$\Delta J = 1$, yes	E1
$^1S_o \rightarrow ^3P_2$	$\Delta J = 2$, yes	M2
$^1S_o \rightarrow ^5S_2$	$\Delta J = 2$, no	E2
$^1S_o \rightarrow ^5D_2$	$\Delta J = 2$, no	E2
$^1S_o \rightarrow ^5D_1$	$\Delta J = 1$, no	M1

the central-force approximation, only the first of these can occur. The cross section calculated by Flowers and Mandl was found to be similar in shape to their electric dipole cross section, but had its peak at about 50 MeV and was only one-hundredth of the magnitude of the former.

Gunn and Irving have argued that the high (γ,n) and (γ,p) thresholds relative to the total binding energy of He^4 will make the (γ,pn) and $(\gamma,2p2n)$ disintegrations predominant except near the threshold, because of the greater phase-space available. Specific calculations for the four-body break-up yielded a cross section rising to a maximum of several millibarns. Experimental evidence on this reaction is very scant, but results for $He^4(\gamma,pn)H^2$, although not entirely consistent, do not confirm such a large cross section.

2.4 Sum Rules

An alternative approach to the calculation of the photon absorption cross section is afforded by an extension to the nuclear case of the Thomas-Reiche-Kuhn sum rule of atomic physics. This is a quite general quantum-mechanical result whose classical analogue is the fact that the area under the absorption curve for a charged simple harmonic oscillator depends only on its mass and charge, and not on its natural frequency. The sum rules for matrix elements refer to a summation performed over all possible final states, giving a result dependent on the wave function of the ground state only. For electric dipole absorption by any system of Z protons and N neutrons, irrespective of its dyn-

amical nature, the result of Levinger and Bethe (1950) is

$$\sigma_{int} = \int_0^\infty \sigma(E)dE = (2\pi^2 e^2 \hbar/Mc).(NZ/A) = 0.060(NZ/A) \text{ MeV barn.}$$

This result assumes only that the forces between nucleons are "ordinary", and should be obeyed by any detailed model which neglects exchange forces. The inclusion of exchange forces unfortunately requires a specific model. Using an independent particle model, Levinger and Bethe included the effect of a fraction x of (purely central) exchange forces in the neutron-proton interaction, and the result was to increase the sum by the factor (1 + 0.8x). Correlation effects between the nucleons, completely ignored in such a model, would increase this factor.

On the basis of the same statistical model Levinger and Bethe also gave an expression for the quantity

$$\sigma_b = \int_0^\infty (\sigma/E)dE,$$

the integrated cross section weighted by the dE/E approximation to the bremsstrahlung spectrum; this is a quantity which may be readily compared with measured bremsstrahlung yields. The result (again for electric dipole absorption) may be written

$$\sigma_b = (4\pi^2/3).(e^2/\hbar c)\left\{NZ/(A-1)\right\}R^2$$

where R is the root mean square radius of the nuclear charge

distribution (in the ground state). Foldy (1957) has pointed out that this should hold rigorously for the lightest nuclei H^2, H^3, He^3 and He^4 independently of the possible existence of inter-nucleon correlations, but assuming only that the ground state wave functions are space-symmetric. He showed that this assumption was valid for these nuclei, and derived the above expression on its basis alone.

At energies not far above the giant resonance, experimental measurements of integrated cross sections for heavy nuclei are generally consistent with the dipole sum, with $x \sim \frac{1}{2}$ in agreement with the results of neutron-proton scattering experiments. The electric dipole character of the resonance is thus demonstrated. For lighter nuclei σ_{int} comes out lower than the sum rule values, even with $x = 0$, unless the integration is carried well above the resonance, indicating a high-energy "tail" in the excitation function. For He^4 ($N = Z = A/2$), the Levinger-Bethe value is 84 MeV mb for $x = 0.5$. Assessing the experimental results then available*, Rustgi and Levinger (1957) obtained the value 124 MeV mb. They derived a sum rule on the basis of Irving's wave function for the He^4 ground state, including tensor

* Later results, together with the present experiment, indicate a slightly smaller discrepancy.

forces, which led to lower values: between 86 and 102 MeV mb for various standard Majorana-Heisenberg exchange force mixtures.

These authors were less successful in calculating σ_b for He^4 in this way, obtaining the value 1.23 mb. This was seriously in error compared with the experimental value of 2.7 mb. The corresponding value of $R = 0.99 \times 10^{-13}$ cm also disagreed with that of 1.61×10^{-13} cm obtained by high-energy electron scattering experiments (McAllister and Hofstadter 1956). Levinger and Bethe, and Foldy, pointed out that this result can be deduced by including the effect of the finite r.m.s. radius of the proton, but the discrepancy in σ_b remains, and must cast further doubt on the correctness of the Irving wave functions.

2.5 Angular Distributions

The distribution of events in terms of the angle, measured in the centre-of-mass system of coordinates, between incoming and outgoing particles in any nuclear reaction provides information about the angular momentum and parity properties of the nuclear levels involved. In a photonuclear reaction (or its inverse, radiative capture) the most useful information concerns the multipoles emitted or absorbed in

the radiative process.

Scattering theory gives the differential scattering cross section (per unit solid angle) for a collision process as proportional to an infinite series of terms $C_i P_i(\cos\theta)$, where $P_i(\cos\theta)$ are the Legendre Polynomials in terms of the centre-of-mass scattering angle θ, and C_i are real coefficients. In the case of processes of the form

$$A + a \rightarrow C^{*} \rightarrow B + b,$$

where C^{*} is a compound nucleus in a state having definite angular momentum and parity, only terms involving even powers of $\cos\theta$ are finite. The differential cross section may then be written in the form

$$\frac{\sigma(\theta)}{\sigma(\pi/2)}\, d\Omega = (1 + C_1\cos^2\theta + C_2\cos^4\theta + \ldots)d\Omega,$$

for comparison with experiment. The coefficients $C_1, C_2, \ldots$ are now complicated functions of the energy of the incident particle, the various angular momenta (orbital and spin) and the nature of the interaction forces involved. The highest power occurring, $\cos^{2L}\theta$, is restricted by the smallest of l_1, l_2 and J_o, where l_1 and l_2 are the orbital angular momenta of initial and final systems, and J_o is the angular momentum of the intermediate state. The restriction may be expressed:

$$L \leqslant l_1,\ L \leqslant l_2 \text{ and } L \leqslant J_o.$$

If the compound state is a mixture of levels of opposite parity, or if the incoming and outgoing waves contain mixtures of opposite parity, interference terms in odd powers of cosθ may be involved.

Perry and Bame (1955) have listed the angular distributions expected for the reaction $H^3(p,\gamma)He^4$, for all possible interaction states producing electric dipole, magnetic dipole or electric quadrupole radiation. The $^1P_1$ state, which is principally responsible for electric dipole emission, has $J_o = 1$, and so only terms up to $\cos^2\theta$ may appear--in fact $(1 - \cos^2\theta) = \sin^2\theta$ in this case. $^1D_2$ (giving electric quadrupole radiation) has $J_o = 2$, leading to a distribution of the form $(\sin^2\theta\cos^2\theta)$. A $(\sin^2\theta\cos\theta)$ term arises from the interference of radiation from these two states; the resulting forward asymmetry is the most striking experimental evidence for the presence of quadrupole absorption. $^3S_1$, with $l = 0$, must give rise to an isotropic distribution. The other triplet states produce terms having the same powers of cosθ, but with more complicated coefficients. All these results should hold also for the inverse reaction $He^4(\gamma,p)H^3$, as θ is the same angle in both cases.

For photodisintegration in heavy nuclei, with many overlapping levels in the intermediate state, the interpret-

ation of angular distributions is less complete. Electric dipole and quadrupole absorption characteristically give $\sin^2\theta$ and $\sin^2\theta\cos^2\theta$ distributions, with interference, but an isotropic emission of particles can now be the result of evaporation from the compound nucleus, or from internal scattering of the particles in the nucleus, and does not necessarily imply magnetic dipole absorption.

3 PHOTODISINTEGRATION OF HELIUM: REVIEW OF EXPERIMENTAL WORK

3: PHOTODISINTEGRATION OF HELIUM: REVIEW OF EXPERIMENTAL WORK

3.1 The Experimental Data of Interest

An ideal photodisintegration experiment would yield complete excitation functions for all possible reactions, so that the total radiation absorption cross section curve could be obtained by addition, at the same time allowing comparisons to be made between the various individual reactions.

In practice, one frequently has to be satisfied with much less than this. The commonest difficulty arises from the use of electron accelerating machines producing heterogeneous beams of high-energy γ-rays, with the result that the energy distribution of the emitted particles will not be related in a simple way to the excitation function. With light nuclei such as helium, this problem is reduced by there being no excited state accessible to any of the particles present; the calculation of the energy of the

responsible photon becomes a matter of particle dynamics only. If two-body disintegration can be assumed, complete knowledge of the momentum of each product is more than enough information for this purpose, and a check is frequently available. Concerning multiple reactions it is more frequently necessary to draw rather indirect conclusions.

Where a detailed excitation function cannot be deduced, its integral can be used to arrive at a value of the integrated absorption cross section. Again, where the photon energy is experimentally limited, a measured "yield" may have to be confined to a finite energy range smaller than that required to cover the entire reaction region. Yields measured with bremsstrahlung beams can be conveniently compared with theoretical sum rules using the bremsstrahlung weighted cross section of Levinger and Bethe mentioned in section 2.4.

Sometimes the energy at which a reaction or total cross section curve has its maximum value may be estimated experimentally; such resonance energies can be distinguishing characteristics of different theoretical predictions. Reaction thresholds are not generally so valuable in photodisintegration studies, since they are readily calculable from more accurate nuclear mass measurements, but they might be used for identification purposes. (A well established

photonuclear reaction threshold makes a convenient calibration point for a betatron energy scale.)

An angular distribution (in centre-of-mass coordinates) for the emitted particles is desirable, as well as its variation with photon energy, so that information may be deduced on the mode of γ-ray absorption at various energies. This is more easily obtained for protons than for neutrons, since most devices for measuring the energy of a proton will automatically indicate its direction of emission as well. In the case of helium, the photoneutron angular distribution is derived by detecting the recoil He^3 particles.

When the target nucleus breaks up into more than two parts, it is useful to be able to measure the degree of correlation between the emitted particles, and the relative angles at which they are emitted. This will be possible only with a device like a cloud chamber, with which the assignment of two or more charged particles to a common reaction can be positively made, or with the aid of a coincidence counting technique. This type of study is particularly important at fairly high energies, where the Levinger pseudo-deuteron model might be expected to describe the process.

3.2 Photodisintegration Experiments

3.2.1 General

In the last decade, the photodisintegration of helium has been studied experimentally by a number of workers. These experiments have all involved the use of helium gas targets in betatron or synchrotron bremsstrahlung beams, and the reactions have been investigated by means of the direct detection of one or more of the disintegration products; this has mostly been done by measuring charged particle tracks in cloud chamber photographs or photographic emulsions, though the use of counters has also been reported.

The results of these various experiments will be discussed under the heads of the different experimental techniques employed.

3.2.2 Cloud Chamber Experiments

In spite of the difficulties attending the use of a Wilson expansion chamber in the X-ray beam from an accelerating machine (Atkinson et al. 1957), this instrument is particularly suited to the study of photonuclear reactions in a gas, like helium, of low atomic number. The low stopping power and the relative lightness of the particles involved mean that reasonably long tracks can be obtained, even of the heavier "recoil" particle, and fairly accurate range measure-

ments made. In addition, these events can be easily distinguished from spurious events occurring in heavier gases like oxygen present in the chamber in small proportions.

This small stopping power does have the potential disadvantage that very few particles will complete their range within the sensitive region of a cloud chamber of normal size; but in the case of two-body disintegrations in helium, it is possible to determine the energy release from the measurement of angles alone, though this method becomes rather inaccurate at certain energy regions. Particle momenta can be measured from the curvature of the tracks in a strong magnetic field. Probably the most valuable feature of the technique is the fact that the site of the reaction can be readily identified and the product particles leaving it easily distinguished; against this must be set the undoubted drawback of the considerable time and labour involved in amassing sufficient data to be statistically significant, and here the particularly small cross sections of helium add to the difficulty.

The first helium photodisintegration experiment was performed by Gaerttner and Yeater (1951), who used a cloud chamber at atmospheric pressure in the beam of a 100-MeV betatron. They selected as helium events those "flags" and

"singles" with recoil tracks longer than was possible from carbon or oxygen reactions, and drew some approximate conclusions on the relative sizes of the integrated cross sections of the (γ,p), (γ,n), $(\gamma,2d)$, (γ,pn) and $(\gamma,2p2n)$ processes by comparing the various yields with those from carbon, nitrogen and oxygen reactions. They gave an angular distribution (based on about 120 photoproton events) which was compatible with $\sin^2\theta$; this fact, together with an estimate of the integrated absorption cross section which appeared to exhaust the dipole sum, was taken as evidence in favour of electric dipole absorption as the predominant mode for the helium nucleus. A rough energy distribution based on about the same number of (γ,p) events had a peak between 25 and 30 MeV, with the average photon energy estimated as (27 ± 2) MeV. Above 30 MeV, the method of computing the photon energy by measuring the momentum in the forward direction became very inaccurate.

Nicolai and Goldwasser (1954) confined themselves to a brief investigation of the contribution from photons above the threshold for meson production, and compared the numbers of events with machine runs at 135 and 300 MeV. They also published integrated cross section estimates comparable with those of Gaerttner and Yeater.

Matheson et al. (1954) reported a cloud chamber experiment using 285-MeV bremsstrahlen, but no results have been published.

The first attempt to use the cloud chamber method to obtain a reasonably detailed cross section curve was by Reid, Swinbank and Atkinson (1956). Running at 340 MeV, these authors determined the forward momentum and hence the γ-ray energy for a number of (γ,p) events, and again found the accuracy inconveniently low at energies over 30 MeV. The cross section curve appeared to fall off rather rapidly beyond the peak near 26 MeV, and the angular distribution was symmetrical, but narrower than $\sin^2\theta$. Main and Reid (1957) determined the form of the (γ,n) cross section over a limited range of energies between 40 and 70 MeV by measuring single He^3 recoil tracks, and found it to be smoothly decreasing. (No correction was applied for loss of events from the useful region of the chamber; range measurements are necessary here, since the neutron leaves no track.)

The most comprehensive study of the photodisintegration of helium so far undertaken has been reported by Gorbunov and Spiridonov (1957, 1958a and 1958b). Using a 170-MeV bremsstrahlung beam and a magnetic field for particle momentum measurement, they examined 9,000 cloud chamber photographs and identified over 2,500 events of each of the

reactions (γ,p) and (γ,n), as well as smaller numbers of the other processes. They gave energy distributions based on the analysis of over 700 each of (γ,p) and (γ,n), and 91 (γ,pn) events.

These results permitted the first direct comparison of (γ,p) and (γ,n) cross sections measured in the same experiment. Gorbunov and Spiridonov concluded that these were essentially similar; the (γ,n) curve was slightly higher than the (γ,p) above 35 MeV, but it is possible that the difference was a result of large momentum corrections or of neglected multiple scattering. Both curves had peaks just under 2 millibarns high in the energy region 27-28 MeV, and the half-width (measured from the proton curve only, since neutron measurements did not extend below 27 MeV) was about 15 MeV, a fairly large value. However, it was not found possible to fit the measured curves satisfactorily by means of any of the published theoretical curves for electric dipole absorption, even neglecting absolute values and trying to fit the shape alone. In addition, the r.m.s. α-particle radius calculated from σ_b when the contributions from all the reactions were added agreed with the electron scattering value, rather than the value calculated from the various wave functions tried by Gunn and Irving.

The angular distributions showed marked differences. The neutron distributions were apparently identical for photon energies above and below 30 MeV, being almost purely $\sin^2\theta$ functions. This was taken to indicate that there could be no electric quadrupole component in the absorption, owing to the zero effective charge of the neutron. The (γ,p) angular distribution, on the other hand, indicated that E2 absorption sets in around 30 MeV, and that there is increasing dipole-quadrupole interference above this energy. Both distributions could be explained without using any isotropic (magnetic dipole) component. From the fact that proton and neutron distributions were quite dissimilar the conclusion was drawn that the quasi-deuteron process was quite unimportant for the two-body reactions, even at high energies.

For yield and angular distribution measurements on the (γ,pn) reaction, an extra 14,000 photographs, taken at a beam energy of 260 MeV, were examined. Results for this process showed that the quasi-deuteron mechanism was the dominant one at all energies: proton and neutron showed a marked degree of correlation, and had angular distributions similar to those obtained with free deuterons. The fraction of helium disintegrations taking the form (γ,pn), although rising to at least 30% in the region 75-170 MeV, did not appear

to dominate the scene in the way predicted by Gunn and Irving, and only one-tenth as many cases of (γ,2p2n) were found.

A technique whereby very complete information can be gained from any recorded event has been devised by Reid and Lalovic (1960), who used proton scintillation telescopes to trigger a 1.5-atmosphere chamber. The result was selective photography of disintegrations in which at least one proton, of energy 80 to 120 MeV, was emitted. The experiment was run at 330 MeV in an attempt to test the quasi-deuteron hypothesis in detail, but statistics were poor for helium, and the findings, though positive, were based on just 28 events in this element.

3.2.3 Electronic Counter Experiments

Although the counting of β-particles from radioactive product nuclei was among the most important of the techniques used in the first photonuclear reaction studies, the use of electronic methods of particle detection is unsuited to the direct study of processes of such low probability, and few experiments have been reported in which emergent photoparticles have been counted in this way. Moreover, energy determinations tend to be insufficiently precise, and the simultaneous determination of both direction and kinetic

energy, which is such a useful feature of the particle track methods, is difficult where the particle energy is fairly low. In contrast, coincidence counting techniques can play a unique part, notably in the search for simultaneous neutron-proton pairs from quasi-deuteron processes at high energies.

Benedict and Woodward (1951), with a 300-MeV bremsstrahlung beam, counted helium photoprotons of three energy values selected by absorption, using scintillation telescopes fixed at angles of 60° and 90°. Assuming that no deuterons were being counted, and that only the (γ,p) process was responsible for protons, they estimated differential cross section values for this reaction at the chosen energies.

Using direct photoneutron detection in BF_3 counters, with a high-pressure helium target and a 25-MeV beam, Ferguson et al. (1954) derived a partial excitation curve for the (γ,n) reaction by bremsstrahlung subtractions. The peak occurred around 24 MeV, and had a height of approximately 1.3 mb.

Barton and Smith (1958) showed that, for high-energy photodisintegration, nearly all proton emissions are accompanied by simultaneous neutrons, the quasi-deuteron mechanism apparently being the important one. Their method was to detect protons in a specified direction and

energy range, in coincidence with neutrons whose direction alone was specified.

3.2.4 Photographic Emulsion Experiments

The continuous sensitivity and high stopping power of the highly concentrated, fine-grain emulsions developed for charged-particle detection have meant that the role of the photographic technique in photonuclear studies has been a major one. The method is ideally suited for the very low counting rates involved, and track measurement is quicker, and statistical accuracy normally greater, than with cloud chambers. With careful processing, nuclear emulsions will allow easy discrimination between particles of different charge, and different masses can be sorted out by grain-counting at the ends of the tracks.

In the case of helium, there is no possibility of "loading" the emulsion with the target material, but for this nucleus the mechanics of two-body break-up are such that a fairly complete picture can be obtained by studying a single charged particle; for the (γ,n) reaction, loading would give no more information than this in any case.

The first author to report an experiment of this kind was Kikuchi (1952) whose primary investigation was

photomeson production at helium nuclei, using a 320-MeV beam. His proton energy spectra, tabulated for angles of 45°, 90° and 135°, were statistically poor, but he was able to make some broad comparisons with the results of a similar experiment on deuterium.

An attempt to study the (γ,p) reaction in some detail between the threshdd and 40 MeV, with a helium target at atmospheric pressure and a betatron of variable energy, was made by Fuller (1954). Assuming initially that no other reaction was producing particles of charge 1 with comparable frequency, he made no attempt to distinguish between protons and tritons, but used the high-energy end of his "proton" spectrum (where no tritons could be present) to work out a triton distribution to subtract from the other end. A curve was drawn for the (γ,p) excitation function, using proton spectra for four different beam maxima to estimate its shape in the low and high energy regions. This curve had its maximum at 25-26 MeV, just under 2 millibarns high. Theoretical cross section curves were compared, and that of Gunn and Irving found to be more satisfactory than the Flowers and Mandl result, though neither was good. σ_{int} was given as 0.016 MeV barn up to 40 MeV. Rustgi and Levinger (1957) have reported that a monitor recalibration led Fuller to increase

his cross section estimates by 20%.

The shapes of the low-energy ends of the two higher-energy distributions were interpreted by Fuller as indicating that the (γ,pn) cross section is of the same order of magnitude as that of (γ,p) in the region of 30 MeV photon energy, which is in accordance with the prediction of Gunn and Irving, but which was not corroborated by the later findings of Gorbunov and Spiridonov. Fuller placed the peak of the (γ,pn) cross section at about 32 MeV.

Angular distributions were drawn for protons in three different photon energy intervals, and fitted with curves of the form $A + B(1 + C\cos\theta)\sin^2\theta$. The constant term was sensibly zero below 26 MeV, but thereafter increased rapidly with energy, while the "interference" cosine term remained more or less constant. Errors in the values of the coefficients A and C were quite large, the distributions being based on no more than a few hundred tracks each.

In an experiment again designed for studying meson photoproduction, de Saussure and Osborne (1955), with a helium tank at 1 atmosphere and a 350-MeV beam, detected charged particles with $Z = 2$ in under-developed emulsions. Working solely in an angular range where, on dynamical grounds, no He^4 particles (recoiling from π^0 - production)

could be found, they were able to derive a cross section curve for the (γ,n) reaction from the He^3 recoils, over the approximate photon energy range 40 to 125 MeV. For this purpose a form of angular distribution had to be assumed, and they used the pure $\sin^2\theta$ function implied by measurements below the meson threshold. These measurements were statistically poor, and no correction was made for motion of the mass centre. The cross section curve obtained (falling smoothly from about 0.5 to 0.1 mb) was generally higher than that later found by Gorbunov and Spiridonov.

3.3 Radiative Particle Capture

3.3.1 Detailed Balance

Knowledge of photodisintegration cross sections for light nuclei can be increased in some cases by consideration of the appropriate inverse reaction. For any pair of nuclear reactions $A + a \rightleftharpoons B + b$ there exists a very general relationship between the total cross sections $\sigma(\alpha\rightarrow\beta)$ and $\sigma(\beta\rightarrow\alpha)$ for the reaction proceeding by way of "entrance channel" α and "reaction channel" β, and its inverse. Denoting the intrinsic angular momenta of the particles by I, and assuming that the cross sections are averaged over initial, and summed over final, spin states (the usual experimental

condition), then the Principle of Detailed Balance leads to the equation

$$(2I_A + 1)(2I_a + 1)k_\alpha^2\sigma(\alpha\rightarrow\beta) = (2I_B + 1)(2I_b + 1)k_\beta^2\sigma(\beta\rightarrow\alpha).$$

Here k = (particle momentum)/$\hbar$, calculated for a and b in their respective energy channels α and β.

All the experiments so far reported with He^4 in the final state have been proton capture experiments. If A + a → B + b becomes $H^3 + p \rightarrow He^4 + \gamma$, we have $I_A = I_a = \frac{1}{2}$ and $I_B = 0$, while $(2I_b + 1)$, the "statistical weight" for radiation, has the value 2, since there are two possible directions of polarization. Thus

$$\sigma(\gamma,p)/\sigma(p,\gamma) = 2(k_p/k_\gamma)^2.$$

By means of this relation, the results of proton capture experiments can be used to derive the excitation function for the inverse (γ,p) reaction over the appropriate energy range.

As to the angular distribution, it is obvious that this will be identical in both reactions, provided that the measured angle between proton and photon directions is transformed to the system of coordinates moving with the centre of mass.

3.3.2 Proton-Triton Capture Experiments

The first experimental study of the reaction

$$H^3 + H^1 \rightarrow He^4 + \gamma + 19.8 \text{ MeV}$$

was described by Argo et al. (1950), who detected γ-rays from a tritium target bombarded by monoenergetic protons from a 2.5-MeV Van de Graaf accelerator. They gave an estimate of the general shape of the cross section curve, and described the angular distribution by a function of the form $(A + B \sin^2\theta)$, with A small but not zero. These authors claimed to have detected the existence of an excited level around 22 MeV in He^4, but this was not confirmed by Falk and Phillips (1951), who extended the measurements up to 3.4 MeV proton energy. Their value of the constant term in the angular distribution was higher than the previous one. A direct measurement of the γ-ray energy was made by Rochlin (1951), with a magnetic pair spectrometer. He stated that it was probably monoenergetic, and made a yield comparison with the 17.6-MeV γ-ray from $Li^7(p,\gamma)Be^8$. The result was seriously discrepant with a similar comparison by Argo et al.

Willard, Bair and Kington (1953) went up to a proton energy of 5 MeV, and found that the γ-ray yield curve flattened out above 3 MeV, while its slope at lower energies was less than that indicated by previously reported values,

which were already divergent. In this experiment no angular distribution was measured. Warren and Griffiths (1953) verified that this was similar to previous measurements, as was the γ-ray energy, but their absolute yield figure added more doubt on its true value.

The experiment reported by Perry and Bame (1953 and 1955) is the most valuable to date. It consisted of a series of 90° cross section measurements made at energies lower than the (p,n) threshold, with a tritium gas target and NaI scintillation counters. The excitation curve found had the same general shape as that of Willard, Bair and Kington, and Perry and Bame found no evidence for any sharp resonance structure in the curve. Rather, it appeared to have the form of the broad maximum predicted in the theoretical papers.

When the inverse photodisintegration cross section was deduced from these results, broad agreement was obtained with the excitation function as measured by Fuller (though no comparison could be made with his most reliable region, above 25 MeV photon energy); Gorbunov and Spiridonov (1957) subsequently provided further agreement.

Perry and Bame derived their absolute cross section curve from the measurements made at 90°, by assuming a pure $\sin^2\theta$ angular distribution; the departure from this form was

investigated at a series of energies. Adopting the function $(1 + b \cos\theta)^2 \sin^2\theta$, the value of b was found to increase steadily from about 0.02 to about 0.12 as the proton energy rose from 0 to 6 MeV. Any isotropic term in the distribution was demonstrated to be very small, possibly zero, by measuring the yield at 0^o. This is in accord with the picture of predominant singlet-state interaction, at least at these relatively low energies, though Perry and Bame point out that their extrapolated b is about twice Fuller's equivalent value. They are unable to contribute anything to the higher energy region, where Fuller's rapidly rising isotropic term predicts a triplet-state contribution not supported by Gorbunov and Spiridonov.

3.4 Summary

It has been experimentally established that the form of the photon absorption cross section curve is the broad resonance which was predicted by both theoretical papers on the subject; some authors have claimed fine structure for it in the form of sharp resonances, but this has not been supported by any of the direct photodisintegration measurements, nor by the more recently published p-t capture work.

The exact shape of the excitation function is not so well established, beyond the conclusion that it is not the one given by either theory. In particular, the two principal (γ,p) experiments--those of Fuller and of Gorbunov and Spiridonov--result in different widths for the peak.

The (γ,n) reaction has received less attention in the resonance region. The only evidence on its similarity or otherwise to the (γ,p) cross section was adduced by Gorbunov and Spiridonov, who found small differences above the resonance, which have not been established to be genuine. Otherwise the two cross sections appear to be nearly identical, as in theory they should be.

It has never been questioned that the predominant interaction involved is electric dipole absorption of photons, which gives $\sin^2\theta$ angular distributions; there is evidence in the (γ,p) process for electric quadrupole absorption, detected by interference terms of the form $\sin^2\theta\cos\theta$, but how its importance varies with photon energy is in some doubt. The question of possible triplet-state interactions--principally magnetic dipole absorption giving an isotropic component in the angular distribution--is even more doubtful, largely owing to the impossibility of measuring such a small effect

in anything but a very accurate angular distribution--and all those so far published have been lacking in statistical accuracy.

The role of multiple reactions in the total absorption process is another uncertain feature, with Fuller's measurements apparently supporting Gunn and Irving's prediction of a very high cross section, and Gorbunov and Spiridonov finding a completely different state of affairs. The difficulty in this case is one of sorting out the protons from several reactions occurring simultaneously.

The work described in this thesis represents an attempt to clear up some of these uncertainties. Using the photographic emulsion technique, a photoproton energy distribution has been measured for photon energies below 35 MeV, and this evidence will be discussed in relation to the (γ,p) cross section in this energy region; an angular distribution, statistically better than any hitherto published, has been determined from the same data.

From measurements on recoil He^3 nuclei, the (γ,n) cross section has been measured between 40 and 60 MeV, and a corresponding angular distribution obtained. Also, long-range proton tracks have been examined and conclusions drawn

on the ratio of the (γ,p) and (γ,n) cross sections in the doubtful energy region; the contribution to the total absorption cross section of the (γ,pn) reaction is also discussed in the light of these measurements.

4 EXPERIMENTAL METHOD

4: EXPERIMENTAL METHOD

4.1 Method of Plate Exposure

The experimental work performed by the author of this thesis consisted of the examination of nuclear research plates on which had been recorded the tracks of charged particles arising in the photodisintegration of helium nuclei. A brief description is necessary of the method by which the plates had been exposed to this radiation.

The apparatus used was designed, and has been described, by Livesey (1956). It consisted essentially of a cylindrical steel chamber containing the helium gas target at pressures up to 6 atmospheres, with a relatively thin aluminium window at each end for the passage of a narrow bremsstrahlung beam. The beam was that of the 70-MeV synchrotron at Queen's University, Kingston, Ontario, and was collimated by lead blocks, 14 inches thick, before reaching the camera. The photographic plates were placed (in the gas) round the

beam in pairs, in such a way that particles ejected from the irradiated column of gas reached the plates at fairly small angles with respect to their own planes. The use of gases at high pressure is a means of achieving satisfactory reaction yields in elements of low atomic number, while it also permits the suppression of low-energy tracks where necessary.

The geometrical disposition of the plates relative to the X-ray beam, and the relevant dimensions, are shown in Fig. 1. The need to use a containing cylinder of finite length, terminated by metal windows, meant that the plates had to be masked from radiation reaching them from directions making small and large angles with the beam. This was done by having cylindrical brass shields fitted to the end plates of the camera, and surrounding the beam everywhere except for a column 5 inches long at the centre. By excluding from measurement tracks other than those making angles between 25° and 155° with the beam, a source in the irradiated column of gas could be assumed; in practice, only tracks between 35° and 145° were considered reliable.

The emulsions employed were all of the Ilford G2 type, which is sensitive to protons over a wide range of energies, while giving fairly good discrimination between short-range protons and α-particles. All were 200 microns

Figure 1

Arrangement of photographic plates
with respect to the X-ray beam

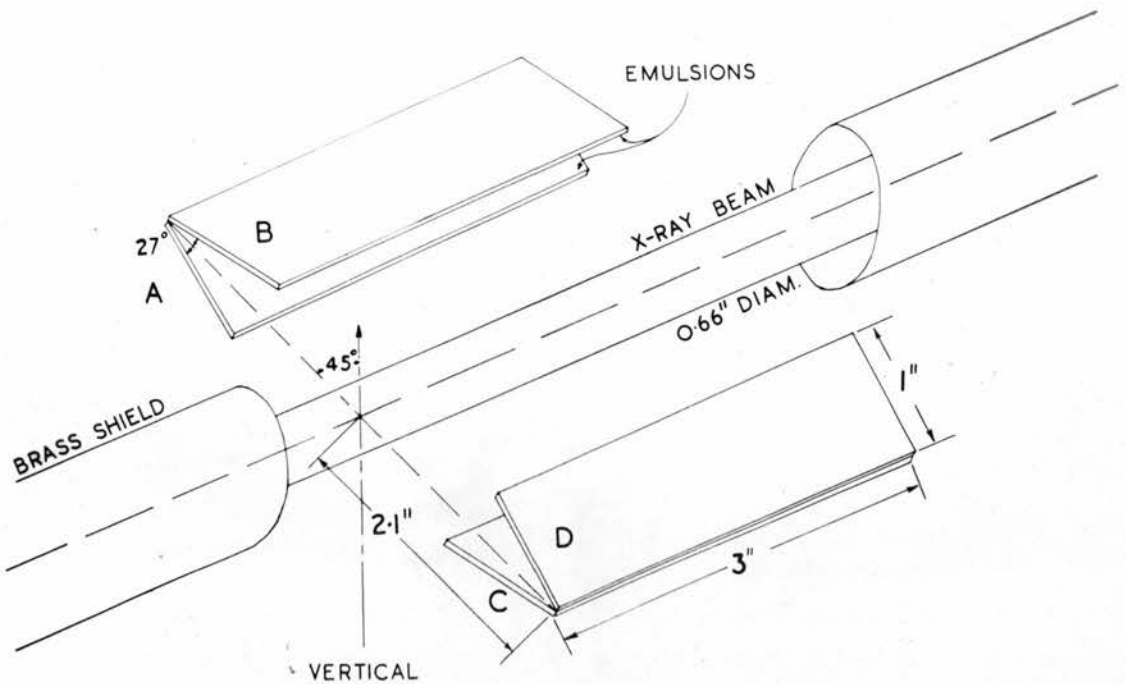
EMULSIONS
27°
B
A
X-RAY BEAM
0·66" DIAM.
45°
BRASS SHIELD
1"
2·1"
D
3"
C
VERTICAL

thick (except for one of 400 microns used for studying long-range protons) and were coated on plates measuring 3 inches by 1 inch. They were processed by the method described by Dawson and Livesey (1956); this procedure involves glycerine treatment before drying, to restore the shrunken emulsion to approximately its original thickness.

The plates studied were obtained in two sets of runs: one set with the synchrotron giving an X-ray beam of its maximum energy, 70 MeV, and one in which the energy was reduced to half. The efficiency of this kind of machine falls rapidly as the energy to which the electrons are accelerated is reduced from its designed value, so that the exposures at 35 MeV were several times longer than those at 70 MeV, for the same nominal dose of X-rays.

In the plates exposed at 70 MeV, to assist identification of the tracks of He^3 particles, radioactive α-particles were introduced into the emulsion. This was achieved by evacuating the camera and placing a weak source of Actinium A, B and C at the centre for half an hour. To identify these tracks positively, the plates were reversed in their holders when this was done, so that all He^4 tracks appeared to come from the "wrong" direction when the plates were later examined under the microscope.

4.2 Principles of the Method

When helium is bombarded with photons of all energies below the meson threshold, the following reactions may be expected to occur, giving rise to the charged particles indicated on the right:

(1) $He^4 + h\nu \longrightarrow H^3 + H^1 - 19.8$ MeV; p,t

(2) $He^4 + h\nu \longrightarrow He^3 + n - 20.6$ MeV; He^3

(3) $He^4 + h\nu \longrightarrow 2H^2 - 23.8$ MeV; d

(4) $He^4 + h\nu \longrightarrow H^2 + H^1 + n - 26.1$ MeV; p,d

(5) $He^4 + h\nu \longrightarrow 2H^1 + 2n - 28.3$ MeV; p

On the assumption that the technique permits the positive identification of all these products, only reactions (1) and (2) can be identified uniquely by detection of a single charged particle. The detection of a proton alone cannot distinguish between cases (1), (4) and (5), while both (3) and (4) can result in a deuteron track on the plate. Reaction (3), however, is theoretically "forbidden" on the electric dipole approximation, and there is no experimental evidence to show that its cross section is other than negligibly small in comparison with the other processes.

As the main study of the work described here concerns the (γ,p) and (γ,n) reactions (1) and (2), it might be thought that all that needs to be done is to investigate the

recoil tritons and He^3 particles. The latter possibility provides in fact the only way of detecting the (γ,n) reaction directly with plates, and is a feasible one; but particles having the same charge make very similar tracks, and the large numbers of protons present in the emulsions make the task of picking out the tritons exceedingly difficult. The method of grain-counting all the tracks before measuring them would be extremely tedious, and even by this method separation of tritons and protons would be made even more difficult by the presence of deuterons from reaction (4).

Instead, it was decided to rely on proton measurement for information on reaction (1), introducing a correction for the presence in the data of tritons, mistakenly measured as protons; energy considerations may be used to exclude protons from other sources, or one can draw such indirect conclusions about other reactions as appear in the distributions. The main results for (γ,p) are based on plates run at 35 MeV, i.e. only 15 MeV above the (γ,p) threshold. It is permissible to run at the higher energy of 70 MeV for the (γ,n) experiment, since He^3 particles (which are fairly readily distinguishable) can arise in no other way; indeed, a fairly high beam energy is necessary in this case, since the heavier recoiling particle takes away only about one-quarter

of the energy released in the reaction, and the tracks must not be too short for accurate measurement. (The range of He^3 is about one-quarter of the range of H^3 of equal energy.)

Fuller plotted "proton" energy distributions in this way, and subtracted from the low-energy end a distribution calculated on the basis that protons at the other end of the scale were associated with recoil tritons, measured as if they were protons. These triton corrections amounted to the majority of "proton" tracks measured below 22 MeV, and a very considerable fraction of those between 22 and 23 MeV. This large correction had the effect of markedly distorting the shape of the uncorrected proton spectrum below the peak, with consequent uncertainty in the cross section results in this region.

It was considered that this defect is inevitable in the photographic method, and that the technique of measuring protons only and then correcting the results is an unsatisfactory one in the susceptible energy region. Therefore the losses at the low end of the proton spectrum due to the use of a high-pressure target are not a serious drawback in the light of this other problem. The threshold region of the cross section is probably best investigated by a separate run at a low beam energy, and using gas at a lower pressure.

Once the kinetic energy and direction with respect to the photon beam have been determined (in laboratory coordinates) for either reaction product, the energy of the photon causing the disintegration, and the complete momentum of the other particle, can be found by an elementary application of the conservation laws. The possibility of a complete solution of this kind is due to the fact that no three-nucleon particle possesses a bound excited energy state, and all that has to be assumed is that the event is in fact a two-body disintegration of a He^4 nucleus.

Momentum relations are shown in Fig. 2, in which primed symbols represent quantities measured in the centre-of-mass coordinate system, unprimed in the laboratory system. Subscripts 1 and 3 refer respectively to the disintegration products of those mass numbers (proton and triton, or neutron and He^3). The forward momentum $h\nu/c$ communicated by the incident photon is shared by the two product particles in the ratio of their masses, since their velocities in this direction must be the same.

By conservation of energy,

$$h\nu = E_1 + E_3 - Q \qquad (1)$$

where $Q = -19.8$ MeV for (γ,p), or $Q = -20.6$ MeV for (γ,n)[*].

[*] For relevant nuclear masses see e.g. Drummond (1955).

Figure 2

Momentum diagram for photodisintegration of He^4
into products of mass 1 and mass 3,
by photon of energy $h\nu$

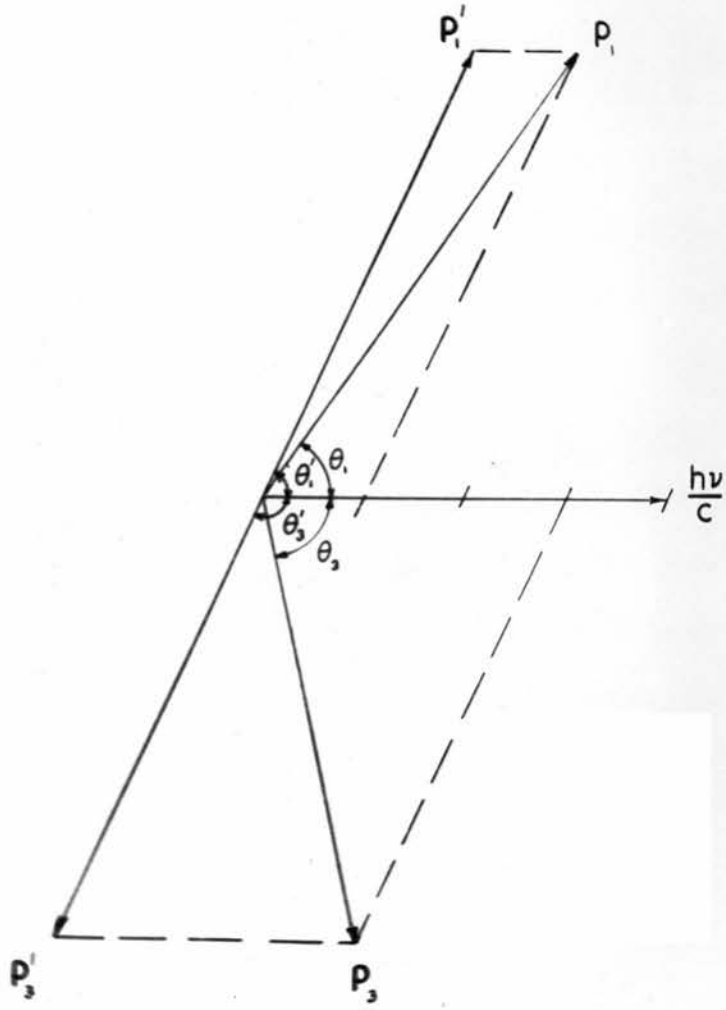
p_1'
p_1
θ_1'
θ_1
θ_3'
θ_3
$\frac{h\nu}{c}$
p_3'
p_3

Applying conservation of momentum parallel and perpendicular to the photon direction, we have

$$h\nu/c - \sqrt{2ME_1}\cos\theta_1 = \sqrt{6ME_3}\cos\theta_3 \qquad (2)$$

and

$$\sqrt{2ME_1}\sin\theta_1 = \sqrt{6ME_3}\sin\theta_3 \qquad (3)$$

Here M is the proton or neutron mass; it is sufficiently accurate to take the recoil mass as 3M.

Square and add equations (2) and (3):

$$(h\nu)^2/c^2 + 2ME_1 - 2\sqrt{2ME_1}(h\nu/c)\cos\theta_1 = 6ME_3$$

We can now use equation (1) to eliminate E_3, giving a relation between E_1, θ_1 and $h\nu$:

$$E_1 = \tfrac{3}{4}(h\nu + Q) - (h\nu/16Mc^2)\left\{h\nu(\sin^2\theta_1 + 1) \pm \sqrt{24Mc^2(h\nu + Q) - (h\nu)^2(\sin^2\theta_1 + 3)}\right\}\cos\theta_1$$

Alternatively, by starting with $h\nu/c$ on the r.h.s. of equation (2), we can eliminate E_1 and relate $h\nu$ to the kinetic energy and direction of the recoil particle:

$$E_3 = \tfrac{1}{4}(h\nu + Q) - (h\nu/16Mc^2)\left\{h\nu(3\sin^2\theta_3 - 1) \pm \sqrt{24Mc^2(h\nu + Q) - 3(h\nu)^2(3\sin^2\theta_3 + 1)}\right\}\cos\theta_3$$

It will be seen that the solutions are not unique. However, one of the answers is excluded in practice by being well outside the experimental energy range, and the positive

value of the square root can be dropped in each case. Values of E_1 and E_3 were computed at different angles for ranges of photon energies of interest here, and used to plot the graphs shown in Fig. 3.

4.3 Microscope Measurements

Particle tracks in nuclear research emulsions can be examined and measured for quite long periods (several hours at a time) by a skilled observer, given a microscope of high optical precision, preferably of the binocular type with inclined eyepieces. For accuracy of measurement, a flat field of view, small depth of focus and an accurate depth gauge are essential, while the motion of the mechanical stage should be precise, to enable the position of any event in the emulsion to be noted with certainty and returned to quickly when required. When the emulsion is used in thick layers, an objective of long working distance is needed.

An instrument embodying the features necessary for this kind of work was developed by Cooke, Troughton and Simms, in accordance with the specification of the Photographic Emulsion Panel of the Cabinet Advisory Committee on Atomic Energy. One of the microscopes used for the measurements to be described was of this type (Model M4005), and is

Figure 3

Showing laboratory energy and direction of He^4 photodisintegration products:

(a) Particle of mass 1

(b) Particle of mass 3

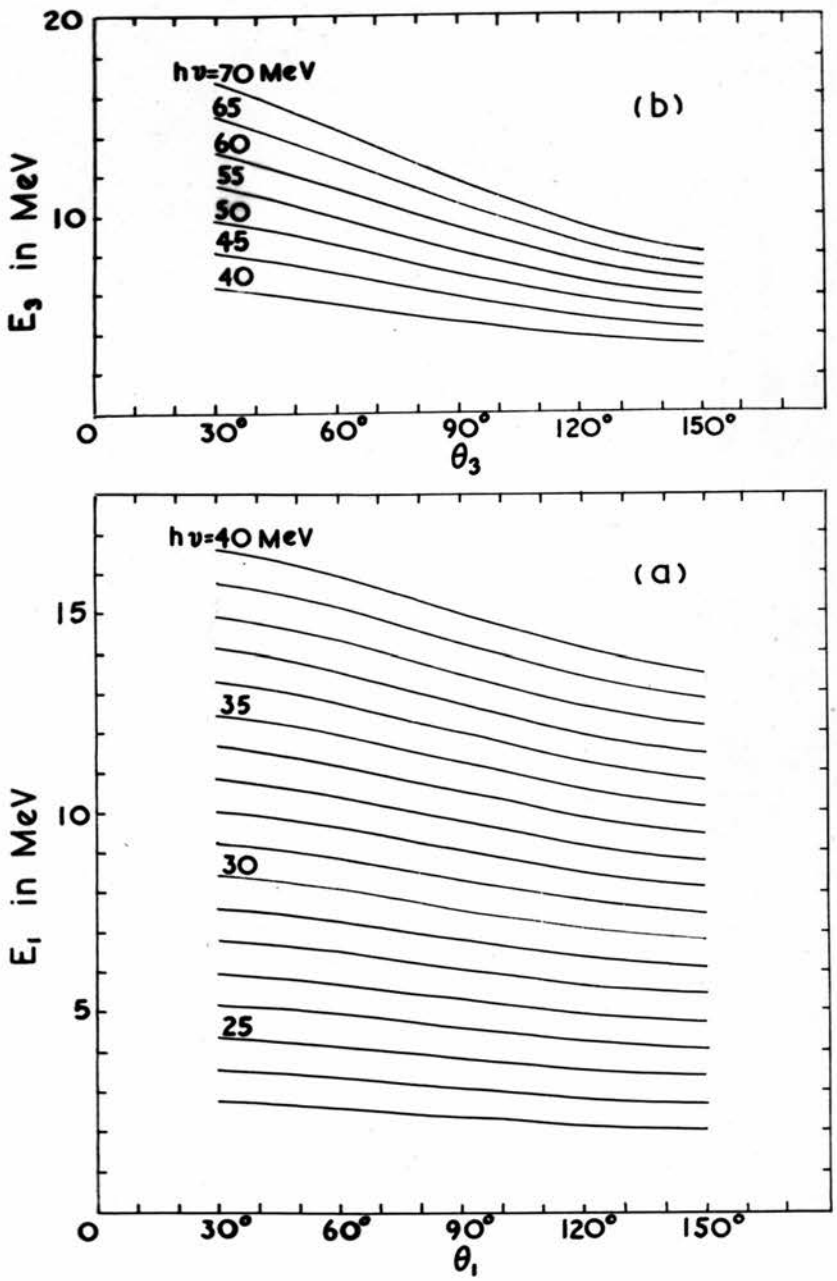
20
10
0
hν=70 MeV
65
60
55
50
45
40
(b)
E3 in MeV
30°
60°
90°
120°
150°
θ3
15
10
5
0
hν=40 MeV
35
30
25
(a)
E1 in MeV
θ1

illustrated in Fig. 4. The microscope has a mechanical stage of special design which permits precise, micrometer-controlled motion over 5 cm in both directions, on ball bearings, and to extend the range of stage movement possible, an orthodox vernier superstage is provided. Illumination (bright or dark field) is built in, and by means of an extensible reflex plate camera, shown mounted on the microscope, photomicrographs can be made whenever necessary.

The other microscope used in the present work was a Cooke, Troughton and Simms Model M10,000. This was adapted by the addition of a binocular head, and a protractor ocular for angular measurements, and was fitted with a simple square stage with vernier scales.

The optical equipment employed in each microscope for both scanning and measurement consisted of a 45x fluorite oil-immersion objective used in conjunction with 10x Kellner eyepieces, giving a field of view just over 0.2 mm in diameter. (Immersion oil has a refractive index very close to that of the emulsions used.) In every case the search procedure involved scanning slightly-overlapping strips of emulsion 0.2 mm apart, each 4.00 cm long and parallel to the 3-inch edge of the plate, i.e. parallel to the X-ray beam; in each field of view the search was carried out through the

Figure 4

Nuclear research microscope

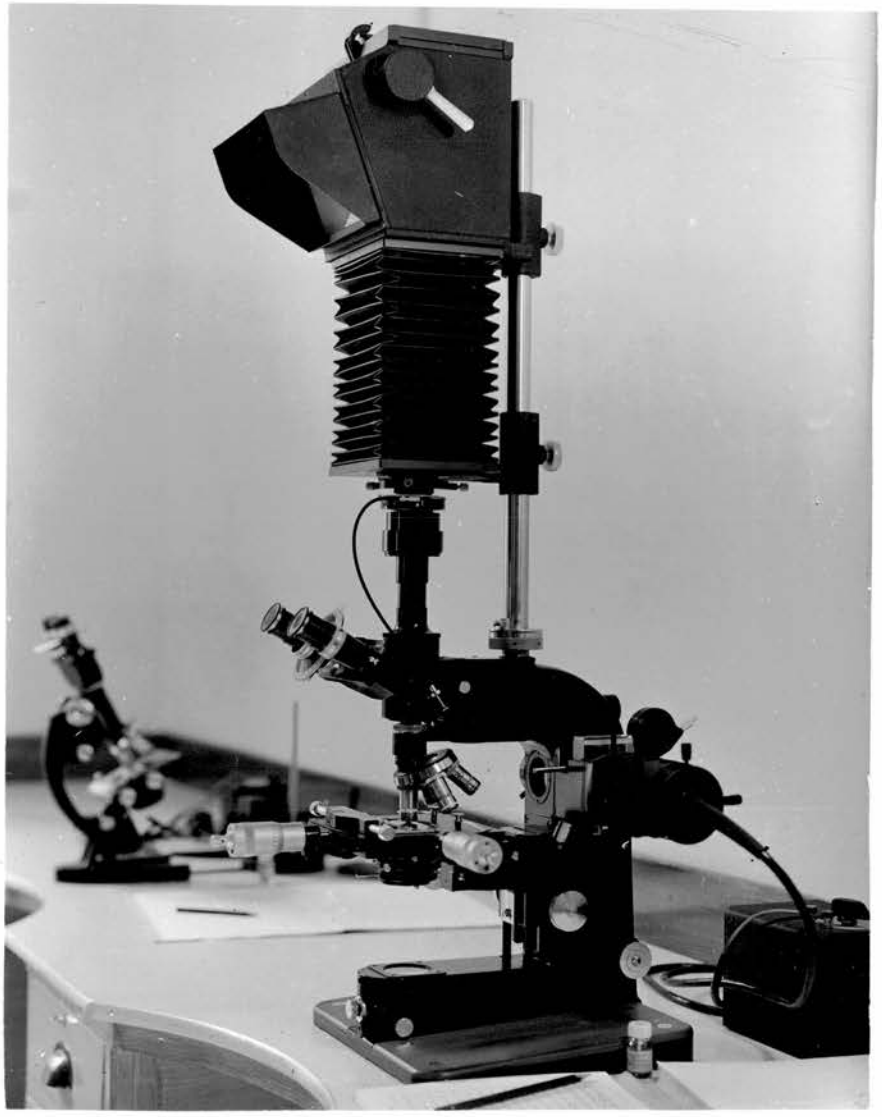

entire depth of the emulsion layer. Every suitable track found was checked to ensure that it had not already been measured in a previous transit, the criterion for acceptance at this stage being that the track was formed by a particle entering the surface of the emulsion within the projected angular range (measured with the protractor ocular with respect to the long edge of the plate) 30° to 150°. Tracks shorter than 16 microns were ignored as being impossible to identify with certainty (in the case of He^3 recoils), or because they lay in the triton-abundant region (in the case of protons).

The information required about each track was its range, and its initial direction in space. The projected range l (measured with a calibrated eyepiece scale) and projected angle ϕ (found by placing the eyepiece cross-hair over the track at its point of entry and noting the reading on the protractor head) had to be taken in conjunction with depth measurements made perpendicular to the emulsion surface, in order to derive the true quantities in three dimensions. When the depth h of the end of the track below the emulsion surface had been measured, by focussing successively on the two planes, the range could be found as

$$R = (l^2 + h^2)^{\frac{1}{2}},$$

while the space angle θ between beam and track was given by*

$$\cos\theta = \cos\phi\cos\delta,$$

$$\text{where } \delta = \tan^{-1}(h/l)$$

The measured quantity h, however, always requires correction before it can be used in this way. Owing to the high bromide concentration of nuclear emulsions, very pronounced shrinkage takes place during the fixing process, so that (if uniformity of shrinkage can be assumed) all vertical measurements will be in error by the factor (final thickness/original thickness). When correction was made for this effect, the "final thickness" taken was that obtained by measuring (with the microscope depth scale) the total depth of the emulsion layer at a standard point, near the centre of the plate; this was done each day. The original thickness had been measured with a mechanical bench gauge just after exposure, but before processing, and was an average of four readings at the corners of the plate. This correction eliminates any errors of calibration of the fine-focus scale from microscope to microscope, giving all depth measurements finally in terms of the same bench gauge, and at the same time allows for the variation from day to day of the emulsion thickness, which is sensitive to ambient humidity.

---

* See Fig. 16 (Appendix).

For the computation of values of θ in large numbers, a method of stereographic projection (Powell, Fowler and Perkins 1959) was found convenient and rapid; the accuracy of about 1° that this method affords was quite sufficient, since the measurements do not warrant greater precision than this. A stereographic net (designed for navigational use) was covered with a sheet of perspex which was free to rotate about the centre of projection; for each track a point was marked in ink on the perspex, on top of the appropriate projected "latitude" δ and "longitude" ϕ. (As dip angles are of one sign only in this calculation, either hemisphere may be used.) The perspex was then rotated until the mark was over the projected "equator" ($\delta = 0$), when the value of θ could be read directly as the line of longitude on which it lay. This is really an application of a more general method for finding the angle between two tracks, with one of the tracks having $\delta = \phi = 0$. By bringing the points for the two tracks to a common great circle, the difference in longitude gives the angle required; in our case the common great circle is always the equator, since one of the points involved is the centre of projection (0,0).

Under favourable conditions, projected ranges could be measured to within one micron, which is the order of mag-

nitude of the original grain size; accuracy was reduced in the case of both very fast protons, whose point of entry into the emulsion was frequently uncertain, and of all tracks more than 100 microns long, which were measured in successive segments. A good microscope carefully used can give equally precise vertical measurements, but distortion of the emulsion introduces errors greater than this.

Tracks showing marked Coulomb scattering along their path were measured by taking separate segments on each side of the bend. Small-angle Coulomb scattering is a much more frequent occurrence in nuclear emulsions, particularly towards the end of a particle's range, and gives tracks their characteristic appearance of being apparently curved. The inaccuracy which this process contributes to range and angular measurements is one of the inherent disadvantages of a method involving track formation in a medium of high stopping power.

Photomicrographs of typical tracks are given in Fig. 5.

4.4 Computation and Assessment of Data

From the recorded data (which included stage references for locating any track again), the range R and space

Figure 5

Photomicrographs of typical tracks from photodisintegration of helium

Upper: Proton track

(Last 0.1 mm: residual energy 3.6 MeV)

Lower: He^3 particle track

(Last 0.1 mm: residual energy 12.5 MeV)

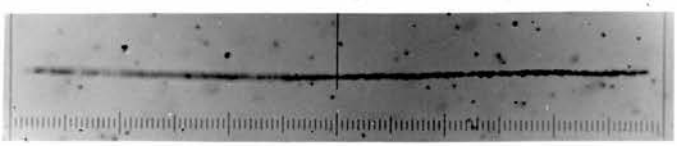

angle θ were calculated for each track in the manner already indicated. Before the range could be used to find the kinetic energy of the ionizing particle responsible, it had to be corrected for the fact that the particle must have lost some of its energy in the high-pressure helium before reaching the plate. The range in the gas is a simple geometrical quantity depending on the direction of the track and its location in the emulsion, and can be converted to "microns of emulsion" and then simply added to the measured range, after multiplication by a factor depending on the pressure and temperature of the gas at the time of the exposure. These quantities had been recorded by the experimenter and used in conjunction with an average stopping power for the appropriate energy range to calculate this factor.

The range in the gas is made uncertain by the finite width of the beam. From Fig. 16 it can be seen that the length of path traversed between the centre of the beam and the point of entry into the emulsion is

$$(y_o^2 + z_o^2 \operatorname{cosec}^2\phi)^{\frac{1}{2}}$$

The possible error in assuming an axial source for all particles is $r.\operatorname{cosec}\theta$; the beam radius r was 0.84 cm in this experiment, and resulted in an error of 0.25 MeV in the energy of the shortest protons measured, at the extreme angles. The

error was more commonly under 0.1 MeV in the lower-energy experiment, and was quite negligible for protons in the 70- MeV run, where a much lower gas pressure was used. On the other hand, He^3 particles from this exposure could have errors of up to 0.3 MeV.

For proton tracks, the kinetic energy was deduced from the corrected range with the help of the combined range-energy relations of Rotblat (1951) and of Gibson, Prowse and Rotblat (1954), these results being applied for particle energies below and above 11 MeV respectively. In the case of He^3 tracks, Rotblat's α-particle relation was used; since the stopping power of emulsion for any particle of a given charge depends only on its speed (Livingston and Bethe 1937), these results can be used for He^3 by simply multiplying both range and energy scales of the graph by the mass ratio $\frac{3}{4}$.

In all cases the combined values of ϕ and δ were examined for consistency; no track was accepted whose direction indicated a source other than in the beam. Genuine tracks occurring farther from the beam (higher values of z_o) will have smaller dip angles δ, but in any case, tracks with large and small values of ϕ must have their dips restricted to smaller values than those with ϕ around 90^o, according to

the relation

$$\tan\delta(\phi) = \tan\delta(\pi/2)\sin\phi$$

(See Fig. 16.) The minimum and maximum allowed values of $\tan\delta(\pi/2)$ were calculated for different values of z_0; graphs of the corresponding minimum and maximum allowed values of δ against ϕ were used to reject from further analysis any tracks then not lying between the relevant pair.

4.5 Analysis of Data

Using the measured values of E and θ, the value of the photon energy responsible for each event was computed by interpolation from the graphs of Fig. 3. To transform from θ to the centre-of-mass angle θ', it was then only necessary to subtract one-quarter of the photon momentum $h\nu/c$ from p_1 (or $\frac{3}{4}h\nu/c$ from p_3), finding the new angle as in Fig. 2. In fact a single θ-θ' relation was plotted for an average value of photon momentum over the range available experimentally, as the angular difference was quite insensitive to changes in photon momentum within these limits. It was thus possible to derive centre-of-mass angles even for those events in which the proton track passed completely through the emulsion, and to include them in subsequent angular distributions. The difference between laboratory and centre-of-mass angles was 2

to 4 degrees for protons, and 6 to 11 degrees for He^3 recoils.

The data were then plotted on a diagram with $h\nu$ and θ' axes, plotting one point for each track, so that energy and angular distributions could be rapidly derived (choosing separate energy regions if need be) simply by counting the numbers of dots within the chosen intervals. The data from different plates were plotted on separate diagrams, to allow comparisons to be made between different observations.

As already explained, the main proton energy distributions were corrected at their lower end by subtracting a suitable triton distribution, calculated on the basis of the high-energy protons found. For a triton of a given energy to interfere with the results, its range has to be such that it could be confused with a proton in the energy region investigated. By ignoring all events below $h\nu = 23$ MeV, it was possible to exclude all but a few of these. For given photon energy values 0.5 MeV apart, corresponding values of $h\nu$ and θ' were calculated for long-range protons whose recoil tritons would be measured as protons giving these values, and after plotting these results on top of the energy-angle diagram the appropriate corrections were found simply by counting dots once more. This correction takes no account of

possible tritons recoiling from high-energy protons which go right through the emulsion; the error from this cause is likely to be small, however, since tracks near $\phi = 90^{\circ}$ are more likely to dip steeply and go through, whereas triton contamination is most serious at extreme backward angles (corresponding to forward proton directions).

Angular distributions had to be corrected for the variation with θ of the solid angle available for the collection of particles by the plate. This solid angle is proportional to $\sin\theta$. (See Appendix.) Again using the approximate independence of photon momentum in the centre-of-mass transformation, it was possible to correct the number of events in each θ' interval simply by dividing by $\sin\bar{\theta}$, where $\bar{\theta}$ is the mean <u>laboratory</u> angle in the appropriate range.

5 RESULTS AND DISCUSSION

5. RESULTS AND DISCUSSION

5.1 Photoprotons (35-MeV Exposure)

5.1.1 General

Two plates were exposed together, with the synchrotron energy reduced to half of its maximum value; these plates occupied the positions marked A and D in Fig. 1. Equal areas of each plate were scanned by two observers, and in the total area of 11.2 cm^2 of emulsion 4,195 proton tracks were measured, of all ranges greater than 16 microns.

When the angles of dip were examined, as explained in section 4.4, about 6% of the tracks from Plate A had to be rejected; this percentage is the sort of figure commonly experienced with the apparatus used, and can be accepted as normal background. However, the number of tracks originally rejected from the Plate D data amounted to 20%, which is suspiciously large and differs markedly from the figure for

Plate A, which ought to give similar results. A further discrepancy in the total numbers of tracks found in the two plates--the ratio was 1.28, the greater number being in Plate D--indicated a pronounced deviation from the supposed symmetry in the original experimental arrangement. The most likely explanation was that the synchrotron beam had shifted in some way during the exposure which, on account of the reduced X-ray flux at the lower energy, had been made on three separate days, with the machine being shut down and started up again each day. (The camera was not touched during the exposure.) As the X-ray beam was produced by the accelerated electrons impinging on a vertical tungsten wire target inside the evacuated "donut", the shift was assumed to be in the vertical direction which means in a direction at an angle of 45° to the plane through the outer edges of the two plates. (See Fig. 1.)

To calculate the amount of vertical shift of the beam that would explain the asymmetry in the data, distributions in dip angle δ were drawn for tracks from sample areas of each plate the same distance from the theoretical beam centre; to simplify the geometrical calculation, only tracks having values of ϕ between 70° and 110° were used, i.e. only those in planes nearly at right angles to the beam.

These dip distributions are shown in Fig. 6; in the scanned regions chosen, no tracks should have had dips outside the range 7° to 36°. A revised upper limit of 44° was selected for Plate D, and the beam shifted by an amount in accordance with this new limit, as indicated in the same Figure. The amount required was 4.5 mm (at the centre of the camera), a shift which would require that the lower permitted limit for δ in Plate D be raised also; however, the observed dip distribution indicates that the beam must have been in its intended position for at least some of the time, though it was probably out of position during most of the exposure. (A plausible explanation is that the beam was in its new position on the second and third days of the run only.) The new angular limits for Plate A also fit the observed distributions well.

To check the estimated shift, the ratio of the new distances of the scanned emulsions from the centre of the beam was measured in the same normal plane, for the new beam position. From Fig. 6, the value is $(R_1/R_2)^2 = 1.33$ approximately, to be compared with the observed yield figure of 1.28. The slightly lower observed value may be taken as further evidence that the beam was in its intended position during the earlier part of the run.

Figure 6

Effect of vertical beam shift on possible range of dip angles in a normal plane; new limits are marked by arrows on observed dip distributions for $70^{\circ} \leq \phi \leq 110^{\circ}$

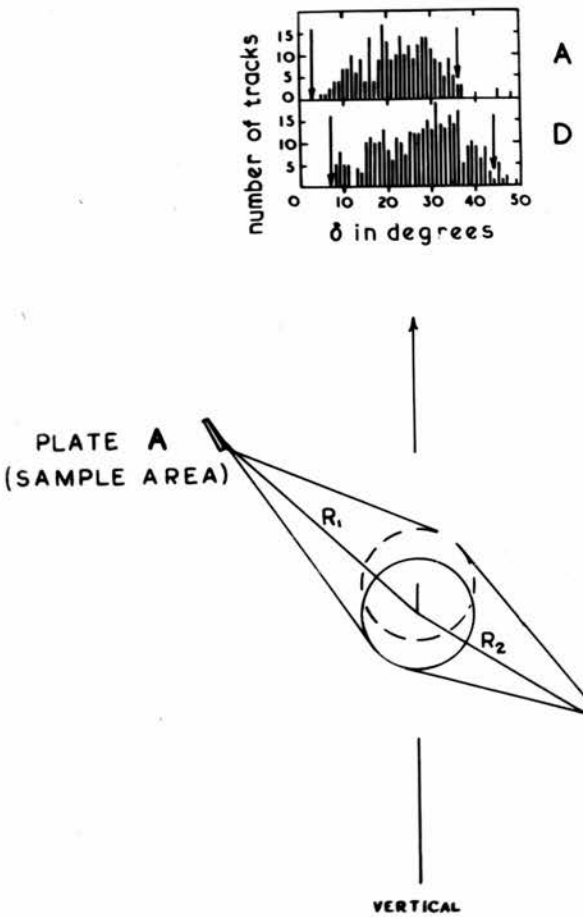
number of tracks
15
10
5
0
A
D
0
10
20
30
40
50
δ in degrees
PLATE A
(SAMPLE AREA)
R1
R2
D
VERTICAL

When the revised criterion of selection was applied to the tracks from Plate D, only 9.5% of these had to be rejected. It is possible that some genuine photoproton tracks have still been excluded by this selection procedure, but it is considered better to apply the procedure rigorously in order to be certain of excluding unwanted tracks, absolute yield values being very uncertain in this experiment anyway. Tracks that were originally excluded from the Plate D data, but later admitted on the basis of the new dip criterion, were initially treated on their own before being included with the other data for final plotting of distributions. In all cases the separate results were broadly similar to one another.

A non-central beam implies different range corrections for the two plates, owing to the different distances from the beam centre. The error in assuming complete symmetry was, however, only a fraction of that owing to the finite width of the beam itself, and was of different sense in the two plates; it was therefore ignored, and the results from the two plates were averaged in all final distributions. When plotted separately, distributions for the two plates exhibited no significant differences.

5.1.2 Energy Distribution

When the photon energy was computed for each acceptable track, there were in all 3,569 tracks arising from (γ,p) reactions caused by photons of energies 23.0 MeV and over. Their distribution in terms of photon energy, plotted at 0.5-MeV intervals, is given in Fig. 7, in which the small shaded histogram is the distribution which has been subtracted to allow for tritons. Tracks that went right through the emulsion, with the result that their total range could not be measured, are not included in the distribution. Most of these tracks were long enough to indicate that they arose from disintegrations at energies over 32 MeV, so that any escape correction would only be appreciable above that energy; there was no significant difference in the distribution obtained by counting only tracks with dip angles below 20°, almost all of which stopped within the emulsion.

The histogram shows no evidence of any significant resonance structure, in accord with previous photodisintegration evidence and with the most recent work on the inverse reaction.

The distribution falls fairly steadily from the peak position to a photon energy just over 30 MeV, after which there is a long "tail" extending beyond 40 MeV, i.e.

Figure 7

Energy distribution of photoprotons from helium: low-energy run. Shaded histogram is recoil triton correction; smooth curve is free-hand estimate of distribution

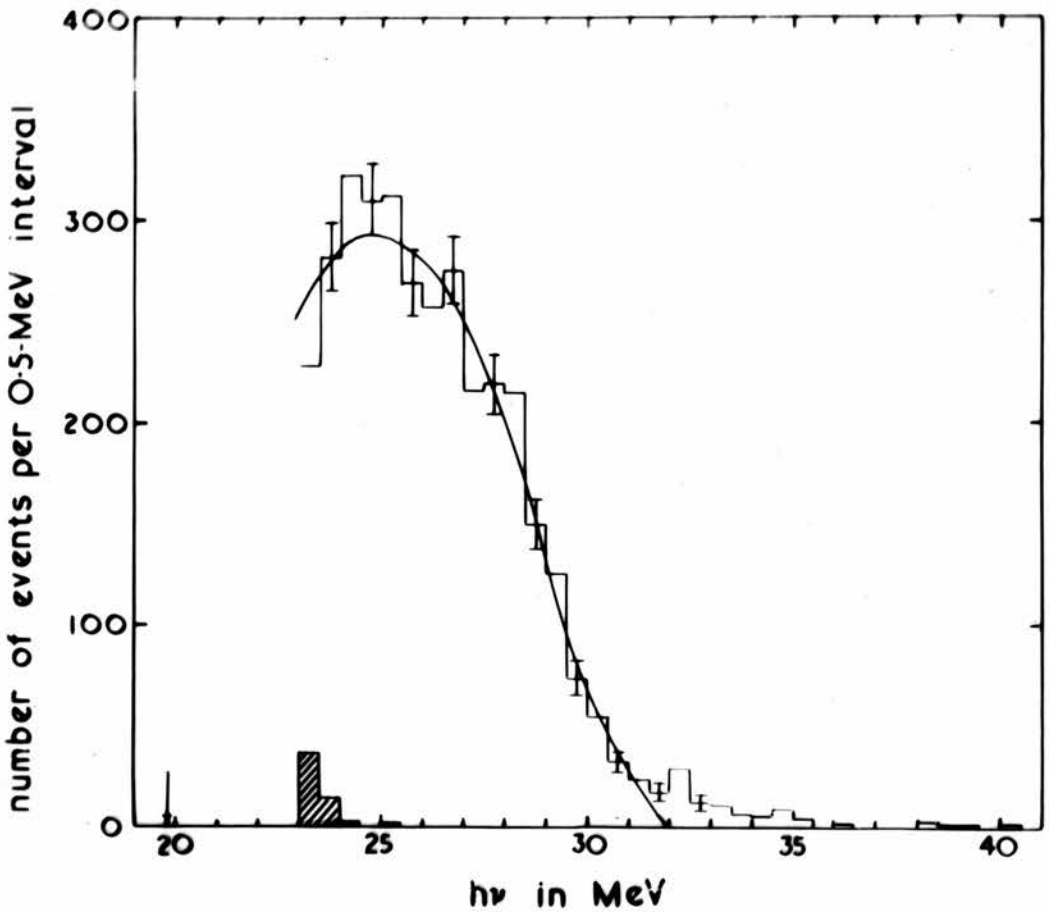
400
300
200
100
0
20
25
30
35
40
number of events per 0·5-MeV interval
hν in MeV

well beyond the nominal maximum photon energy of 35 MeV. In fact it is not possible to assume that the maximum energy was exactly 35 MeV; the method used to reduce the running energy of the machine (reducing the length of time for which the radio-frequency accelerating voltage was applied to the cavity before the X-ray pulse was produced) was itself accurate to about 1%, but the maximum electron energy was not stabilized, and could have varied by ± 2 MeV from the nominal 70 MeV. In addition, temperature changes in the magnet are known to have led to a downward drift by as much as 5 MeV during a long run at 70 MeV (Janzen 1960). Thus the figure of 35 MeV is quite uncertain, and the probable value was several MeV lower. The most satisfactory estimate of the peak energy is obtained by inspection of the distribution itself, and the free-hand curve drawn in Fig. 7 assumes the figure of 32 MeV.

In order to examine the form of the (γ,p) cross section curve, it is necessary to know the flux (in absolute terms if possible) of photons of each energy in the bremsstrahlung beam at the time of the exposure. In the Queen's University synchrotron the beam is monitored by an ionisation chamber which is connected through a direct current amplifier to a chart recorder, thus giving a permanent record of the

relative beam intensity. The total dose in roentgens was calculated in the present instance from a comparison by Janzen (1953) of the monitor reading with that given by a Victoreen "r-meter", with the thimble of the instrument placed behind 7.3 cm of lucite at a distance of 1 metre from the synchrotron target.

The shape of the photon flux curve was taken as that given by the formula of Schiff (1951).* This formula gives a relative intensity spectrum, integrated over all angles, and was corrected to take into account the differential absorption by the Pyrex glass donut, through which the beam passes from the synchrotron target. The resulting spectral shape is in good agreement with an experimental determination at 70 MeV by Goodjohn (1956).

To take into account the fact that different quantities of ionization are produced by photons of different energy, this relative intensity curve was divided by E/J_v (also a function of energy) to give the relative number of roentgens per MeV interval as a function of energy; E is the energy flux per unit area, and J_v is the quantity of ionization produced in the Victoreen thimble per unit volume.

* The constant C in the formula was taken to be 191, after Katz and Cameron (1951).

Values of E/J_v were calculated from the absorption coefficient for X-rays in lucite, the energy required to produce unit ionization in air, and the ratio of the energy loss in lucite to that in air for electrons (Gray 1936).

The ordinates in this last graph were then given absolute values in r/MeV such that the total area under the curve was 1 roentgen. The flux curve was finally obtained by multiplying the ordinates once more by E/J_v and dividing by the energy, to give the number of photons per MeV interval per cm^2 per roentgen, as a function of the photon energy. Representative flux curves are given in Fig. 8; these are almost identical below 25 MeV.

The way in which the observed cross section shape varies when different peak synchrotron energies are assumed is also indicated in Fig. 8, where that portion of the smooth curve of Fig. 7 between 23 and 29 MeV has been divided by the flux curves with maxima at 30 , 32 and 35 MeV. It can be seen that the maximum occurs at about 25½ MeV for the nominal beam setting of 35 MeV, but moves up to 29 MeV when a value of 30 MeV is used. On the other hand, the cross section curve below 25 MeV is virtually unaltered by these changes. The figure of 32 MeV, which seems the most likely one from the appearance of Fig. 7, gives a peak just above 25 MeV on the

Figure 8

(a) Photon flux curves with maximum energies 30, 32 and 35 MeV

(b) Showing the effects of using these flux curves to estimate cross section shape from smooth curve of Fig. 7

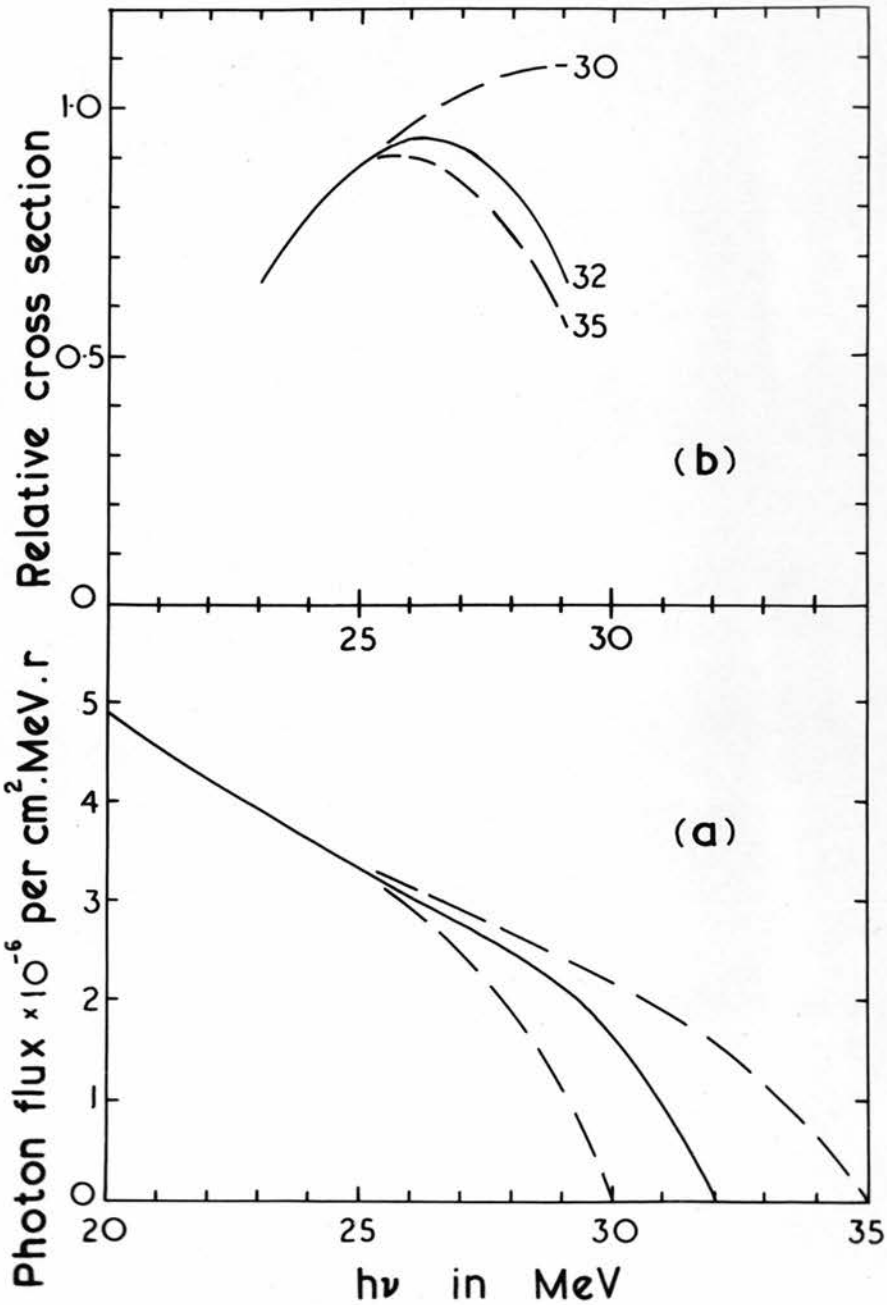
Relative cross section
1·0
0·5
0
30
32
35
(b)
25
30
Photon flux x 10⁻⁶ per cm².MeV.r
5
4
3
2
1
0
(a)
20
25
30
35
hν in MeV

basis of the free-hand curve. This flux curve was selected for the conversion of the histogram to the absolute cross section of Fig. 9.

In ascribing absolute values to the yields and cross sections in this experiment, angular spread of the bremsstrahlung beam has to be taken into account; the beam intensity is not constant at all distances from the axis, but falls off smoothly according to a curve whose width at half-maximum increases as the maximum beam energy decreases. The collimator used in front of the plate camera was narrow enough to ensure that the intensity was effectively constant (at the maximum value) across the aperture, whereas the monitor chamber admitted the full width of the beam. Assuming a Gaussian expression for the variation of beam intensity with angle, it can be shown that the ratio of fractions of the total beam intensity admitted by the camera aperture at 70 and 32 MeV is equal to the square of the inverse ratio of the angular half-widths at these energies, $(\theta_{32}/\theta_{70})^2$.

According to Schiff (1946), the angular spread of the beam should give half-maximum intensity at $\bar{\theta} = mc^2/E_o$, where E_o is the kinetic energy of the electrons. However, the very few experimental measurements that have been made indicate a much larger spread than this, probably owing to

Figure 9

(γ,p) cross section as a function of photon energy, derived from the observed distribution of Fig. 7, using 32-MeV flux curve and beam spread assumption discussed in text

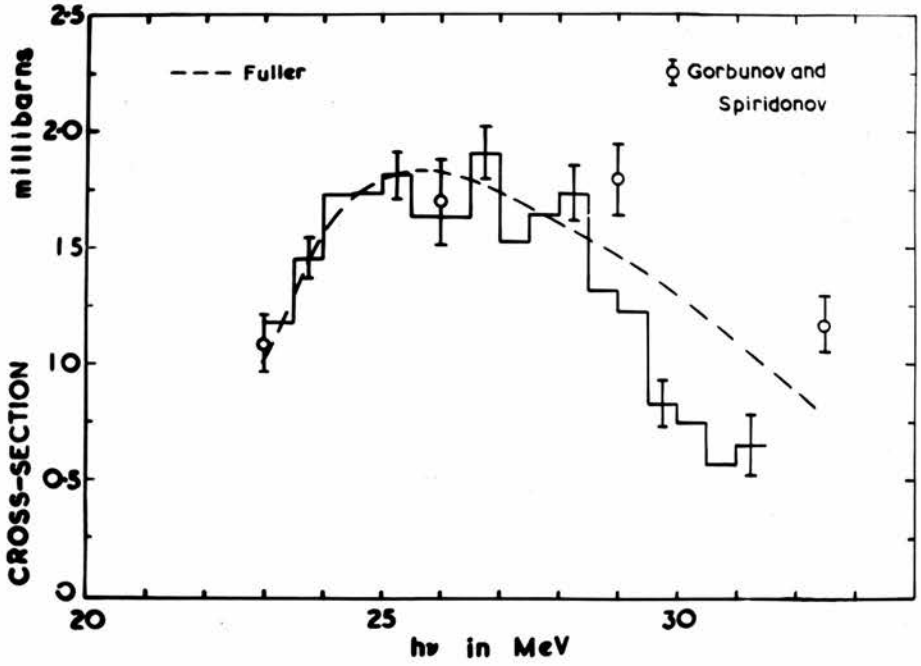
CROSS-SECTION millibarns
2·5
2·0
1·5
1·0
0·5
0
20
25
30
hν in MeV
Fuller
Gorbunov and Spiridonov

electron scattering in the thick targets used. If we adopt the values of 1.4° at 70 MeV (Janzen 1953) and 2.7° at 30 MeV (Mitchell et al. 1953), the flux ratio is $(2.7/1.4)^2 = 3.7$, which is much lower than the theoretical figure of $(70/32)^2 = 4.8$.

The experimental estimates were made on different synchrotrons, and should not be relied upon further than to conclude that the theoretical ratio is probably high. Instead, the figure of 2.5 (lower still) has been adopted here, since it gives cross section values of about the same magnitude as those found by other workers with more accurately calibrated beams. The value of θ_{32} deduced from this assumption and the 70-MeV measurement is 2.2° for the Queen's University machine. Direct measurement of $\bar{\theta}$ as a function of E_o is desirable.

The shape of the cross section (Fig. 9) is similar to the composite curve obtained by Fuller in a series of irradiations. The more rapid descent above 29 MeV should not be given too much weight in the light of the uncertainty in the synchrotron peak energy (See Fig. 8(b)).

The results of Gorbunov and Spiridonov are not sufficiently detailed in the resonance region to allow a

direct comparison, except to note that their values beyond the peak suggest a less rapid fall.

There is no evidence here of any excess of protons at low energies (our more reliable region), such as led Fuller to conclude that the (γ,pn) cross section was substantial around 30 MeV photon energy. The peak in Fuller's 32-MeV energy distribution was less pronounced than that obtained in this experiment (Fig. 7).

5.1.3 Angular Distribution

Fig. 10 shows the centre-of-mass angular distribution, corrected for variation of solid angle, of all proton tracks corresponding to photon energies over 23 MeV; tracks passing right through the emulsion are included, as are all events above 32 MeV. The number of measured events included in the histogram exceeds 3,500; this is statistically the best measurement so far made for helium, and permits detailed examination.

The appearance of the histogram suggests the provisional assumption that there is no appreciable isotropic term in the distribution, since it falls rapidly towards zero at 0° and 180° on each side of the peak, just forward of 90°.

Figure 10

Centre-of-mass angular distribution of 3,569 proton tracks from (γ,p) reactions in He^4 above 23 MeV photon energy; the smooth curve represents the function

$$f(\theta) = B(1 + 0.46\cos\theta + 0.01\cos^2\theta)\sin^2\theta$$

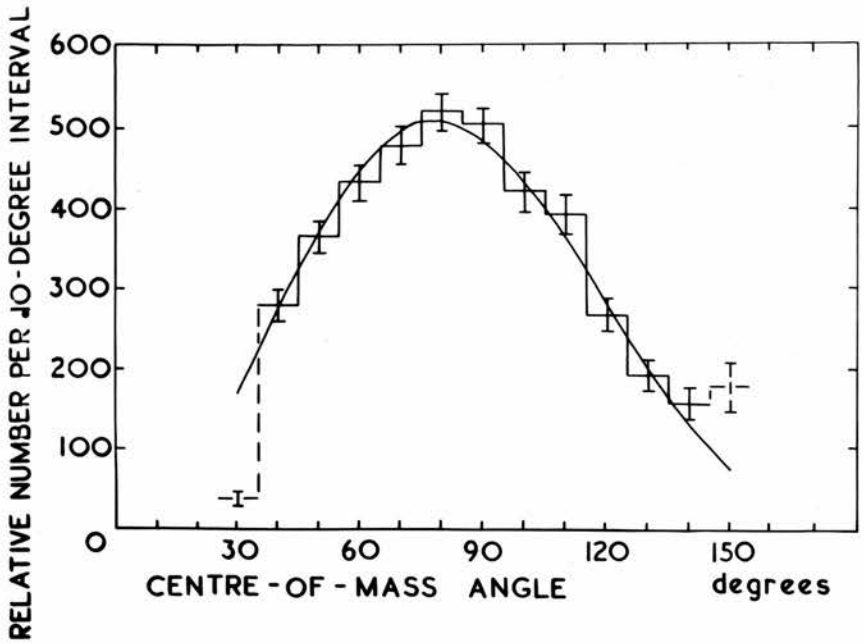
RELATIVE NUMBER PER 10-DEGREE INTERVAL
600
500
400
300
200
100
0
30
60
90
120
150
CENTRE-OF-MASS ANGLE
degrees

Accordingly, the method of least squares was employed to find the expression of the form

$$f(\theta) = B(1 + C\cos\theta + D\cos^2\theta)\sin^2\theta$$

which best fits the observed data. The values obtained for the coefficients C and D were:

$$C = 0.46 \pm 0.05$$

$$D = 0.01 \pm 0.1$$

In Fig. 11, distributions are drawn for the three equal photon energy ranges between 23 MeV and the estimated maximum synchrotron working energy of 32 MeV. The few tracks corresponding to higher energies that this were omitted, since their angular distribution did not appear to follow the general trend but had more events at backward than at forward angles. It is thought that the reason for this may be the reduced efficiency of finding tracks of long-range protons in these plates; a 35-MeV photon produces a proton of 10 MeV in the backward direction, whereas the energy of a proton in the forward direction is almost 13 MeV, corresponding to a 50% increase in range and a considerable reduction in track density.

Setting D equal to zero in the above expression for $f(\theta)$, the least squares method yielded the following values of C, which have been used in calculating the smooth curves

Figure 11

Centre-of-mass angular distributions of protons from (γ,p) reactions in He^4 in photon energy ranges (a) 23 - 26 MeV, (b) 26 - 29 MeV, (c) 29 - 32 MeV; smooth curves represent the functions

(a) $f(\theta) = B(1 + 0.46\cos\theta)\sin^2\theta$

(b) $f(\theta) = B(1 + 0.48\cos\theta)\sin^2\theta$

(c) $f(\theta) = B(1 + 0.47\cos\theta + 0.25\cos^2\theta)\sin^2\theta$

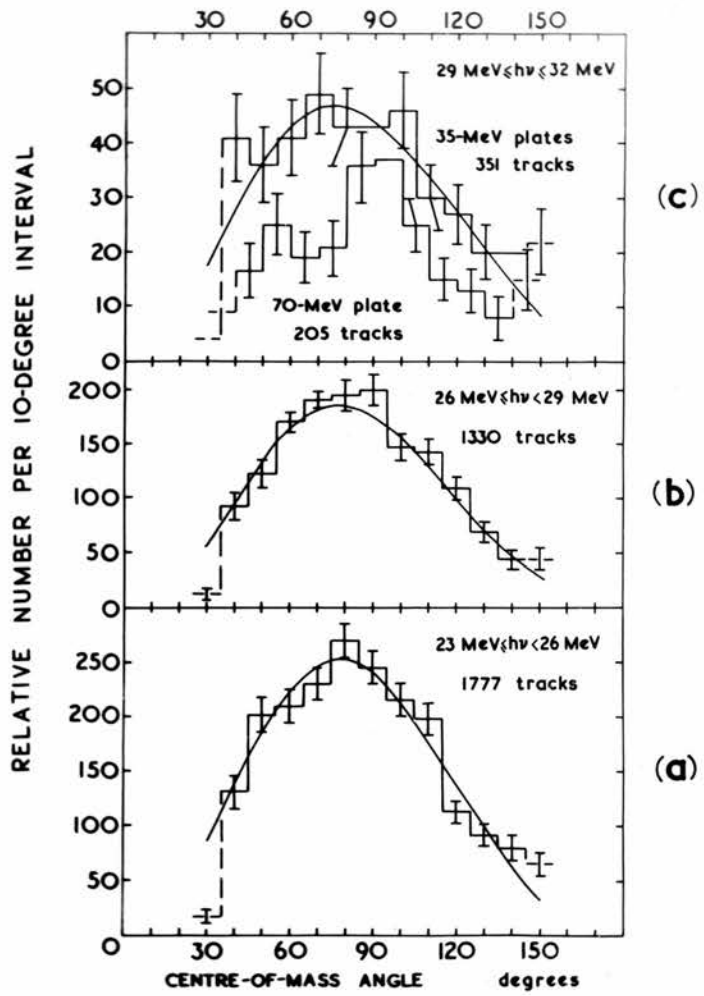
30 60 90 120 150
29 MeV≤hν≤32 MeV
35-MeV plates
351 tracks
70-MeV plate
205 tracks
(c)
26 MeV≤hν<29 MeV
1330 tracks
(b)
23 MeV≤hν<26 MeV
1777 tracks
(a)
RELATIVE NUMBER PER 10-DEGREE INTERVAL
CENTRE-OF-MASS ANGLE degrees

drawn through the histograms:

$23\ \text{MeV} \leq h\nu < 26\ \text{MeV}$: $C = 0.46 \pm 0.03$

$26\ \text{MeV} \leq h\nu < 29\ \text{MeV}$: $C = 0.48 \pm 0.04$

In an attempt to estimate the size of the $\cos^2\theta\sin^2\theta$ quadrupole term at the highest energies, where it would be expected to be greatest, D was allowed to vary; the least squares values obtained in this case were:

$29\ \text{MeV} \leq h\nu \leq 32\ \text{MeV}$: $C = 0.47 \pm 0.15$

$D = 0.25 \pm 0.34$

Examination of the histograms and fitted smooth curves suggests that the addition of a constant term in the angular distribution function--the effect of which would be to raise the tails of the curve at high and low energies but to leave the peak position unaltered--is unnecessary; the value of such a term, if present, is certainly smaller than the error in its determination.

The mechanism indicated by these results is electric dipole absorption of photons modified by some electric quadrupole absorption producing the interference term $BC\cos\theta\sin^2\theta$ in the angular distribution, to an extent not varying appreciably in the energy region investigated here. There may be a small quadrupole term, but its coefficient D has large statistical errors. The absence of any isotropic

component in the distribution means that magnetic dipole absorption is absent, i.e. the proton and triton leave with their spins anti-parallel.

Only three previous attempts have been reported to measure in detail the departure of the angular distribution for this reaction from a pure $\sin^2\theta$ function, for which the predominant electric dipole interaction is responsible. Perry and Bame, in their study of the inverse reaction, made a direct measurement of the γ-ray yield at 0^o to the proton beam, to show that the isotropic component in the angular distribution was very small if not zero. Fuller, extending the investigation to higher energies by direct photodisintegration, fitted his distributions by functions of the form $A + B(1 + C\cos\theta)\sin^2\theta$; he found that the value of C remained fairly constant (if anything, increasing slowly with energy), but was hampered by poor statistics. However, he obtained evidence above 26 MeV for finite values of A, rising to 0.33 ± 0.2 in the energy range 30 to 40 MeV. This appeared to imply an increasingly important magnetic dipole interaction leading to a final triplet state.

Gorbunov and Spiridonov started from the assumption that no such isotropic term existed and fitted their two experimental distributions with the function including the

$\sin^2\theta\cos^2\theta$ term for electric quadrupole absorption. Below 30 MeV they found no significant departure from pure $\sin^2\theta$; their higher energy distribution (which extended right up to 170 MeV) had C = 1 and D = 0.5 approximately.

The present results differ from the previous ones chiefly in the larger value of C obtained; they resemble those of Fuller in detecting little variation in the value of this coefficient with photon energy. The values found by Gorbunov and Spiridonov, being much smaller below 30 MeV and much larger than the present values above, result from the choice of such extended energy ranges for investigation.

5.2 He^3 Particles*

5.2.1 General

Five plates were studied which had been exposed at a beam energy of 70 MeV; a total area of 17.50 cm^2 of emulsion was scanned, and several hundred He^3 tracks identified and measured.

As most of the recoil He^3 particles at this energy have rather short ranges, their tracks were dense and apt to be confused with those of protons, deuterons and particularly

---

* The work described in this section was performed jointly with Dr D. L. Livesey of the University of British Columbia, Vancouver, Canada (Livesey and Main 1958).

tritons, all present in much larger numbers, but unsuitable for grain-counting purposes. For this reason, α-particles had been introduced after the normal exposure, as explained in section 4.1, and a criterion was adopted whereby a track was only measured and analysed as He^3 if it was at least as dense as a nearby track entering the emulsion from the "wrong" direction. The α-particle tracks occurred in most microscope fields and greatly facilitated identification of He^3 tracks. The ionization density in a short He^3 track is very nearly equal to that produced by He^4, and it is considered that although a few genuine He^3 tracks may have been rejected, elimination of triton tracks should have been ensured. In a preliminary investigation, the proportion of He^3 tracks accepted was $(12 \pm 1)\%$ of all tracks exceeding 10 microns in length, in spite of considerable variation (due to deliberate variation of the processing technique) in the density of proton tracks and of the local abundance of control α-particle tracks.

A possible source of error in this particular experiment lay in the occurrence of recoiling He^4 nuclei ejected from the gas by fast neutrons. This had been checked experimentally by measurements of the fast neutron flux, both within the beam and in the region of the plates, and by

counting the number of helium tracks entering one of the plates (not exposed to Actinium α-particles) in the "wrong" direction. The results showed that less than 5% of the recorded tracks could be due to this process. Radioactive contamination could also cause background effects, but no definite α-particles had been detected in an exposure without gas in the chamber. A survey of possible sources of error indicated a maximum systematic error of 10%, but this is in the opposite sense to the errors caused by rejecting too many He^3 tracks.

Working independently, two different observers calculated the photon energy and angle of emission in the centre-of-mass coordinates for acceptable He^3 tracks. All results were broadly similar when compared, and were finally combined. The He^3 energy varies rapidly with laboratory angle for a given photon energy (See Fig. 3); the lowest He^3 energy recorded (4.5 MeV) corresponded to a photon of 45 MeV at the maximum angle of 150°. Accordingly, a correction was applied for the loss of tracks at backward angles for photon energies below 45 MeV. An additional correction for the events occurring outside the useful range of angles amounted to not more than 5% above 45 MeV.

5.2.2 $He^4(\gamma,n)He^3$ Cross Section

Results obtained for the integrated cross sections in different energy regions are shown in Table III, where the standard errors are based on statistical fluctuations only. The different plates and observers gave quite consistent results, and the final mean values were weighted according to the areas of plate scanned.

Table III

Integrated cross sections (MeV mb)

40-45 MeV*	45-50 MeV	50-60 MeV	40-60 MeV
2.57±0.25	2.21±0.25	2.7 ± 0.3	7.5 ± 0.5

Photon flux estimates can be more accurately made at the full machine energy of 70 MeV. The synchrotron monitor in this case had been calibrated in a separate experiment on the activation of copper foils by the reaction $Cu^{63}(\gamma,n)Cu^{62}$. The integrated cross section for this reaction was taken to be 0.60 MeV barn from the threshold up to 70 MeV (Berman and Brown 1954). This figure led to a direct estimate of the photon flux at 18 MeV in the bremsstrahlung spectrum (automatically corrected for beam spread); at all

* Corrected for losses at angles exceeding 110°.

other photon energies the flux ν was calculated by normalizing a Schiff curve to the point fixed at 18 MeV. It should be pointed out that the maximum synchrotron energy was not stabilized at the time of this exposure, and the procedure may not be reliable above 60 MeV; at lower energies the values of ν should be accurate to $\pm$ 10%.

After full allowance has been made for all errors arising in the experiment, the total integrated cross section from 40 to 60 MeV amounts to (7.5 $\pm$ 0.9) MeV mb. In comparison, Nicolai and Goldwasser found a value of 28 MeV mb for the entire energy range up to 135 MeV, and Gorbunov and Spiridonov obtained 19.7 MeV mb between 40 and 100 MeV, but only about 6.8 MeV mb for the (γ,p) reaction between 40 and 60 MeV.

The shape of the cross section curve was found by plotting the data at 2.5-MeV intervals, as shown in Fig. 12. The results were everywhere consistent with a cross section falling smoothly from an estimate of (0.63 $\pm$ 0.10) mb at 40 MeV to (0.25 $\pm$ 0.04) mb at 60 MeV, with a best value of (0.37 $\pm$ 0.04) mb at 50 MeV. The smooth curve in the Figure was fitted to give the best agreement with the integrated cross sections shown in Table III.

Figure 12

Lower: energy distribution of (γ,n) events in He^4

Upper: estimated (γ,n) cross section as a function of photon energy

NUMBER OF EVENTS PER 2·5-MeV INTERVAL
125
100
75
50
25
0
40
50
60
70
PHOTON ENERGY MeV
0·7
0·6
0·5
0·4
0·3
0·2
0·1
0
ESTIMATED CROSS-SECTION
millibarns

This cross section curve agrees closely with the (γ,p) curve of Gorbunov and Spiridonov, which is lower than their (γ,n) data; it also falls more rapidly than the earlier (γ,n) curve of de Saussure and Osborne, and would indicate a closer agreement between (γ,p) and (γ,n) cross sections than has hitherto been found experimentally. (See Fig. 14.)

5.2.3 Angular Distribution

The centre-of-mass angular distribution of the He^3 particles (corrected for solid angle variation) is given in Fig. 13; the centre-of-mass distribution for neutrons will be this histogram reflected about the 90^o ordinate.

The distribution shows a pronounced asymmetry, which is reflected in the relative numbers of events at forward and backward angles; this ratio was found to be 1.4 ± 0.2 for energies above 45 MeV. In the same energy region Gorbunov and Spiridonov obtained the ratio 2.4 for photoprotons, but are in agreement with de Saussure and Osborne in ascribing symmetry to the photoneutron results; de Saussure and Osborne used their laboratory angles untransformed, whereas the correction applied to the present results has the effect of enhancing any forward peak in the He^3 distribution.

Figure 13

Centre-of-mass angular distributions of He^3 particles emitted in (γ,n) reactions in He^4

Upper: all events above 45 MeV;

smooth curve represents the function

$f(\theta) = B(1 + 0.5\cos\theta)\sin^2\theta$

Lower: all events above 50 MeV

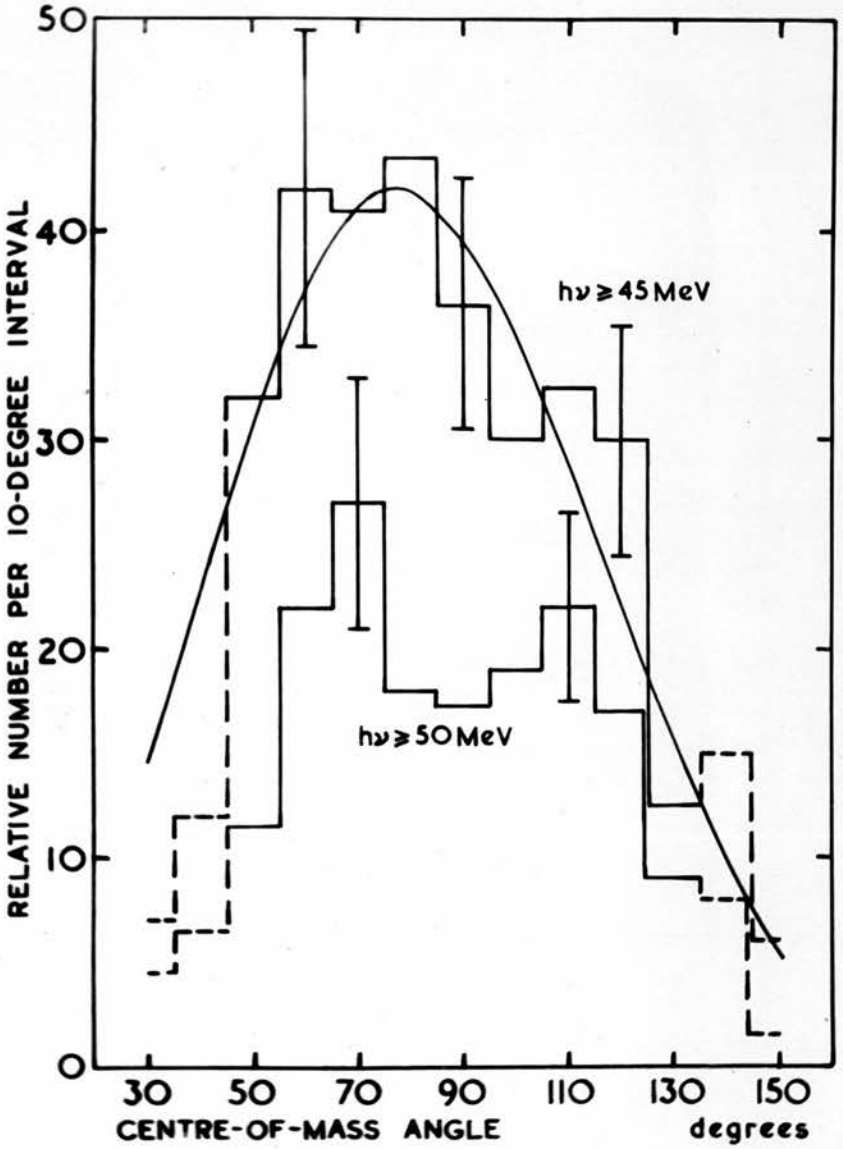
RELATIVE NUMBER PER 10-DEGREE INTERVAL
0
10
20
30
40
50
hν ≥ 45 MeV
hν ≥ 50 MeV
30
50
70
90
110
130
150
CENTRE-OF-MASS ANGLE
degrees

An attempt was made to represent the distribution by a function of the form

$$f(\theta) = A + B(1 + C\cos\theta)\sin^2\theta$$

The best fit was obtained with C approximately equal to 0.5, and the value of A/B did not appear to be significantly different from zero, but experimental errors at the extreme angles, and poor statistics, preclude a real test of the function $f(\theta)$. Gorbunov and Spiridonov agree with the very low value of A/B; de Saussure and Osborne described their distribution (for events between 36 and 84 MeV) by a pure $\sin^2\theta$ function.

The conclusion to be drawn from these results on their own is that the (γ,n) reaction has properties similar to those ascribed to (γ,p) on the basis of other published work; the similarity even appears to extend to the angular distribution, where it has not been found before. Superficially, the result resembles high-energy deuteron photodisintegration, where backward emission of neutrons occurs. However, it has never been suggested that the quasi-deuteron process should be important at energies as low as these.

5.3 Photoprotons (70-MeV Exposure)

The plates exposed at 70 MeV contained tracks of

many photodisintegration products other than He^3 particles from the (γ,n) reaction. The difficulty of sorting out the effects of the various other possible reactions, even if the protons, deuterons and tritons could be distinguished from one another, has been explained in section 4.2.

An examination of the long-range protons can, however, give some information on the importance of multiple processes, and a rough comparison of the (γ,p) and (γ,n) cross sections in the doubtful energy region around 40 MeV. By measuring only tracks longer than 350 microns, tritons should be excluded, and an attempt can be made to estimate the relative importance of the (γ,p) and (γ,pn) processes in producing the protons that remain. Difficulties arise from the very low track density of some of the longest protons in these plates (which had been produced primarily for the study of particles of charge 2), and because their long ranges mean that the tracks are commonly not contained within the thickness of the emulsion used. For the latter reason, attention was restricted to the one plate available with a thick coating (0.4 mm approximately) of emulsion. Even so, many of the protons escaped from the emulsion before completing their ranges, and it is possible that some of these were spurious, since their direction could not always be definitely

ascertained from the appearance of the tracks.

An area of 8.00 cm^2 of the plate was scanned, and some 600 tracks found and measured. In about one-third of the area, measurements were restricted to tracks of protons above 7 MeV kinetic energy (i.e. photon energies over 30 MeV), while in the remaining two-thirds, measurements were extended down to 6 MeV kinetic energy (29 MeV photon energy). The photon energy distribution (corrected for reduction of scanned area below 30 MeV) is given in Fig. 14, on which the region of large escape losses above 36 MeV is indicated.

A very rough comparison of the (γ,p) and (γ,n) cross sections can be obtained from the yields of protons and He^3 particles for photon energies over 40 MeV. For He^3 tracks the yield was $(4.0 \pm 0.6) \times 10^3$ particles per mole of helium per roentgen X-ray dose as measured by the synchrotron monitor. In estimating the photoproton yield, all tracks going right through the emulsion were counted, as well as the stopping tracks above 40 MeV. The lower figure of $(1.8 \pm 0.2) \times 10^3$ protons $mole^{-1} r^{-1}$ can be interpreted as indicating that most of the protons in this region come from the (γ,p) reaction. It should not be taken to imply that the (γ,n) cross section is appreciably higher than the (γ,p) at this point, as suggested by the results of Gorbunov and

Figure 14

Energy distribution of assumed (γ,p) events in He^4 from high-energy run (histogram), and comparison of (γ,p) and (γ,n) cross section determinations beyond the resonance maximum; smooth curve is the best fit of (γ,p) measurements by Gorbunov and Spiridonov

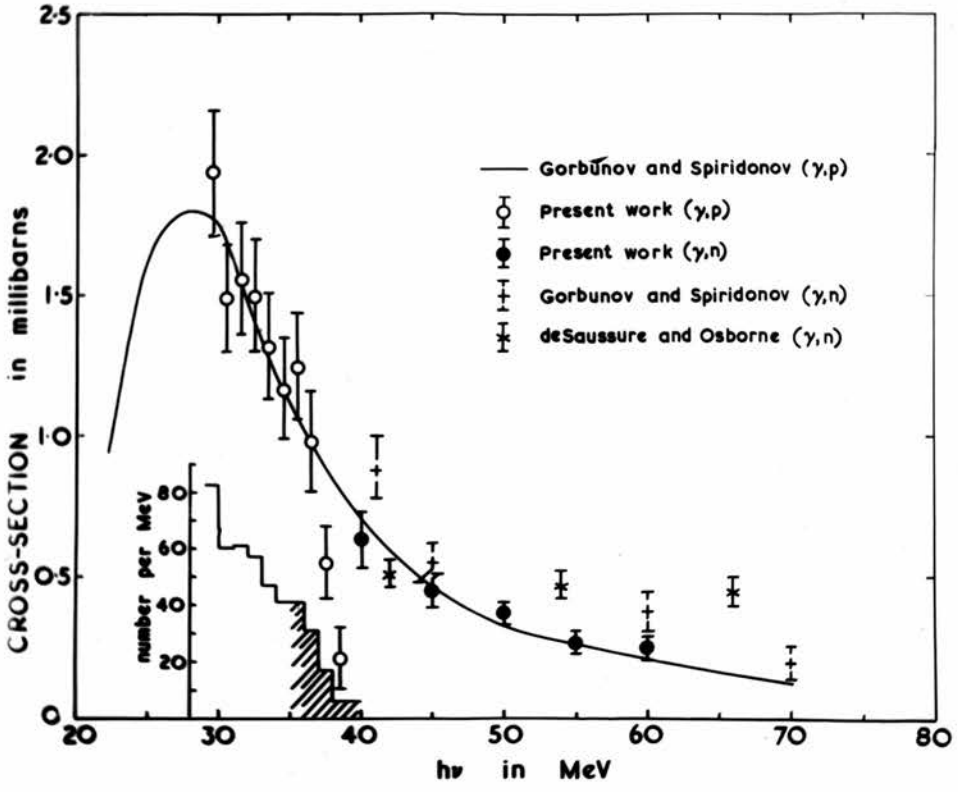
2·5
2·0
1·5
1·0
0·5
0
CROSS-SECTION in millibarns
20
30
40
50
60
70
80
hν in MeV
Gorbunov and Spiridonov (γ,p)
Present work (γ,p)
Present work (γ,n)
Gorbunov and Spiridonov (γ,n)
deSaussure and Osborne (γ,n)
number per MeV
80
60
40
20

Spiridonov, since it is likely that only (γ,p) events up to about 50 MeV were detectable by counting long proton tracks. (The longest track found had a range of almost 2,000 microns, corresponding to a proton energy of 21.1 MeV.) From the results of section 5.2.2 the integrated cross section for the (γ,n) reaction between 40 and 50 MeV is 64% of that from 40 to 60 MeV.

A better idea of the relative sizes of the two cross sections can be gained by examining the forms of cross section curves obtained for the two reactions and attempting to fit them smoothly to one another. For this purpose it is necessary to assume that all the measured protons arise from (γ,p) processes, and to rely on the appearance of the results to indicate if this is not actually the case. There are no monitoring uncertainties in this comparison, since both sets of results were obtained in the same exposure.

The results are illustrated in Fig. 14. It is seen that the (γ,n) points (transferred from Fig. 12) lie close to the (γ,p) curve of Gorbunov and Spiridonov, as do the assumed (γ,p) points, except where escape losses become serious at the high-energy end, and in spite of large statistical errors. There is no indication of excess protons from (γ,pn) processes, even at lower photon energies. The conclusion can

be drawn once more that the (γ,pn) proton contribution is small in the region investigated.

Large statistical errors also mar the angular distribution (Fig. 15); it is hard to say whether the absence of events between 50° and 80° is significant. The distribution for the photon energy region between 29 and 32 MeV is sufficiently unlike the corresponding distribution from the 35-MeV plates (See Fig. 11(c)) to indicate that recoil tritons from high-energy (γ,p) disintegrations may be fairly numerous in this region.

5.4 Summary

The results of the 35-MeV exposure concern the resonance region of γ-ray energies. It was not possible to estimate absolute cross sections accurately, but the shape of the resonance peak was determined, and shown to be essentially similar to that found by Fuller. The present findings differ from Fuller's in requiring no appreciable (γ,pn) contribution of protons for their interpretation. Angular distributions indicate a larger percentage of electric quadrupole absorption than found by previous authors, but show no marked increase with energy of this effect, in the region investigated. No magnetic dipole absorption could be detected.

Figure 15

Centre-of-mass angular distribution of protons assumed to be emitted in (γ,p) reactions in He^4, at photon energies above 29 MeV; smooth curve represents the function

$$f(\theta) = B(1 + 0.5\cos\theta)\sin^2\theta$$

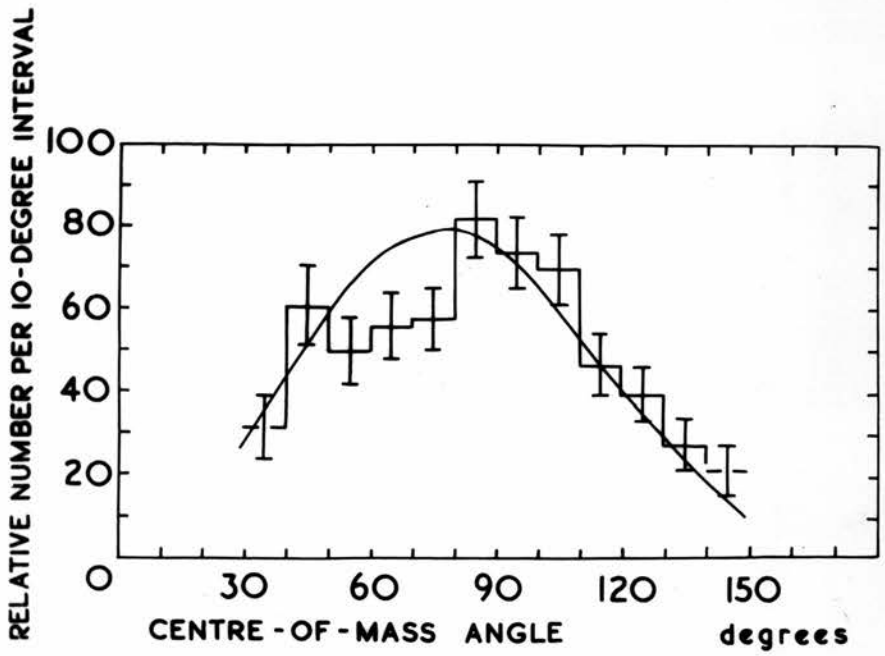
RELATIVE NUMBER PER 10-DEGREE INTERVAL
100
80
60
40
20
0
30
60
90
120
150
CENTRE-OF-MASS ANGLE
degrees

From the plates exposed at 70 MeV, it is concluded that the (γ,p) and (γ,n) cross sections are similar at photon energies over 40 MeV, and that the (γ,pn) cross section is negligibly small in comparison. Asymmetry not previously detected in the neutron angular distribution indicates quadrupole absorption in the (γ,n) process also, or some other unknown mechanism.

ACKNOWLEDGEMENTS

ACKNOWLEDGEMENTS

Of those who have been of assistance during the course of this research, the following deserve particular thanks:

Dr D. L. Livesey of the University of British Columbia, who provided the plates and was generous with encouragement and advice;

Professor B. W. Sargent of Queen's University, in whose laboratory the plates were exposed;

Professor G. D. Preston, who acted as Research Supervisor.

Mrs J. Hodgson, who assisted with computation and photography;

Mrs G. Main, who measured over 3,000 tracks.

The award of a Special Grant of £600 from the Department of Scientific and Industrial Research for the purchase of the nuclear research microscope is gratefully acknowledged.

REFERENCES

REFERENCES

Abraham, G., Cohen, L. and Roberts, A.S. (1955)
Proc. Phys. Soc. A 68, 265

Argo, H.V., Gittings, H.T., Hemmendinger, A., Jarvis, G.A. and Taschek, R.F. (1950) Phys. Rev. 78, 691

Atkinson, J.R., McFarlane, W., Reid, J.M. and Swinbank, P. (1957) Nucl. Instr. 1, 152

Barton, M.Q. and Smith, J.H. (1958) Phys. Rev. 110, 1143

Benedict, T.S. and Woodward, W.M. (1951) Phys. Rev. 83, 1269L

Berman, A.I. and Brown, K.L. (1954) Phys. Rev. 96, 83

Bethe, H.A. and Peierls, R. (1935) Proc. Roy. Soc. A 148, 146

Bohr, N. (1936) Nature 137, 344

Bransden, B.H., Douglas, A.C. and Robertson, H.H. (1957)
Phil. Mag. 2, 1211

Chadwick, J. and Goldhaber, M. (1934) Nature 134, 237

Courant, E.D. (1951) Phys. Rev. 82, 703

Danos, M. (1952) Ann. Phys. 10, 265

Danos, M. (1958) Nucl. Phys. 5, 23

Dawson, W.K. and Livesey, D.L. (1956) Can. J. Phys. 34, 241

Dedrick, K.G.(1955) Phys. Rev. 100, 58

Drummond, J.E. (1955) Phys. Rev. 97, 1004

Falk, C.E. and Phillips, G.C. (1951) Phys. Rev. 83, 468L

Ferentz, M., Gell-Mann, M. and Pines, D. (1953)
Phys. Rev. 92, 836L

Ferguson, G.A., Halpern, J., Nathans, R. and Yergin, P.P.
(1954) Phys. Rev. 95, 776

Flowers, B.H. and Mandl, F. (1951) Proc. Roy. Soc. A 206, 131

Foldy, L.L. (1957) Phys. Rev. 107, 1303

Fuller, E.G. (1954) Phys. Rev. 96, 1306

Gaerttner, E.R. and Yeater, M.L. (1951) Phys. Rev. 83, 146

Gerjuoy, E. and Schwinger, J. (1942) Phys. Rev. 61, 138

Gibson, W.M., Prowse, D.J. and Rotblat, J. (1954)
Nature 173, 1180

Goldhaber, M. and Teller, E. (1948) Phys. Rev. 74, 1046

Goodjohn, A.J. (1956) Ph.D. Thesis, Queen's University,
Kingston, Ontario.

Gorbunov, A.N. and Spiridonov, V.M. (1957)
Zh. Eksper. Teor. Fiz. 33, 21

Gorbunov, A.N. and Spiridonov, V.M. (1958a)
Zh. Eksper. Teor. Fiz. 34, 862

Gorbunov, A.N. and Spiridonov, V.M. (1958b)
Zh. Eksper. Teor. Fiz. 34, 866

Gray, L.H. (1936) Proc. Roy. Soc. A 156, 578

Gunn, J.C. and Irving, J. (1951) Phil. Mag. 42, 1353

Irving, J. (1951) Phil. Mag. 42, 338

Irving, J. (1953) Proc. Phys. Soc. A 66, 17

Janzen, H. (1953) M.Sc. Thesis, Queen's University, Kingston, Ontario.

Janzen, H. (1960) Private Communication.

Katz, L. and Cameron, A.G.W. (1951) Can. J. Phys. 29, 518

Kikuchi, S. (1952) Phys. Rev. 86, 126L

Levinger, J.S. (1951) Phys. Rev. 84, 43

Levinger, J.S. and Bethe, H.A. (1950) Phys. Rev. 78, 115

Livesey, D.L. (1956) Can. J. Phys. 34, 1022

Livesey, D.L. and Main, I.G. (1958) Nuovo Cimento 10, 590

Livingston, M.S. and Bethe, H.A. (1937) Revs. Mod. Phys. 9, 245

McAllister, R.W. and Hofstadter, R. (1956) Phys. Rev. 102, 851

Main, I.G. and Reid, J.M. (1957) Unpublished.

Matheson, W.E., Carlson, C.R., Mathews, P.S., Haxby, R.O. and Whaley, R.M. (1954) Phys. Rev. 96, 826A

Miller, J., Schuhl, C., Tamas, G. and Tzara, C. (1960) J. Phys. Rad. 21, 296

Mitchell, J.S., Smith, C.L., Allen-Williams, D.J. and Braams, R. (1953) Acta Radiologica 40, 463

Nicolai, V.O. and Goldwasser, E.L. (1954) Phys. Rev. 94, 755A

Okamoto, K. (1958) Phys. Rev. 110, 143

Penfold, A.S. and Leiss, J.E. (1959) Phys. Rev. 114, 1332

Perry, J.E. and Bame, S.J. (1953) Phys. Rev. 90, 380A

Perry, J.E. and Bame, S.J. (1955) Phys. Rev. 99, 1368

Powell, C.F., Fowler, P.H. and Perkins, D.H. (1959)
"The Study of Elementary Particles by the
Photographic Method" (Pergamon Press), p. 90

Rand, S. (1957) Phys. Rev. 107, 208

Reid, J.M. and Lalovic, B. (1960) Proc. Phys. Soc. 76, 65

Reid, J.M., Swinbank, P. and Atkinson, J.R. (1956)
Physica 22, 1142A

Rochlin, R.S. (1951) Phys. Rev. 84, 165L

Rotblat, J. (1951) Nature 167, 550

Rustgi, M.L. and Levinger, J.S. (1957) Phys. Rev. 106, 530

de Saussure, G. and Osborne, L.S. (1955) Phys. Rev. 99, 843

Schiff, L.I. (1946) Phys. Rev. 70, 87L

Schiff, L.I. (1951) Phys. Rev. 83, 252

Steinwedel, H. and Jensen, J.H.D. (1950)
Z. Naturforsch. 5a, 413

Szilard, L. and Chalmers, T.A. (1934) Nature 134, 494L

Warren, J.B. and Griffiths, G.M. (1953) Phys. Rev. 92, 1084A

Wilkinson, D.H. (1956) Physica 22, 1039

Wilkinson, D.H. (1959) Ann. Rev. Nucl. Science 9, 1

Willard, H.B., Bair, J.K. and Kington, J.D. (1953)
Phys. Rev. 90, 865

APPENDIX

APPENDIX: THEORY OF MEASURED TRACK ABUNDANCE

Refer to Fig. 16, wherein Cartesian axes are chosen so that the emulsion surface lies in the x-z plane, the forward beam direction being parallel to the x-axis and in the positive sense. Consider an elementary length Δx of the beam (a cylinder of radius r, so small that all particles may be assumed to start at the axis), and a small area $\Delta A = \Delta x' \Delta z$ of the emulsion surface.

The number of particles entering ΔA from the elementary volume $\pi r^2 \Delta x$ (i.e. at angle θ with the forward direction of the beam) will be

$$(\pi r^2 \Delta x).N.\nu.\sigma(\theta).\Delta\Omega$$

where N = number of helium nuclei per unit volume,

ν = incident photon flux per unit area (integrated over time), and

$\sigma(\theta) = (d\sigma/d\Omega)_\theta$ is the differential cross section per unit solid angle at angle θ, for the disintegration process giving rise to the particles being counted. The solid angle

Figure 16

Geometric relations in nuclear plate camera

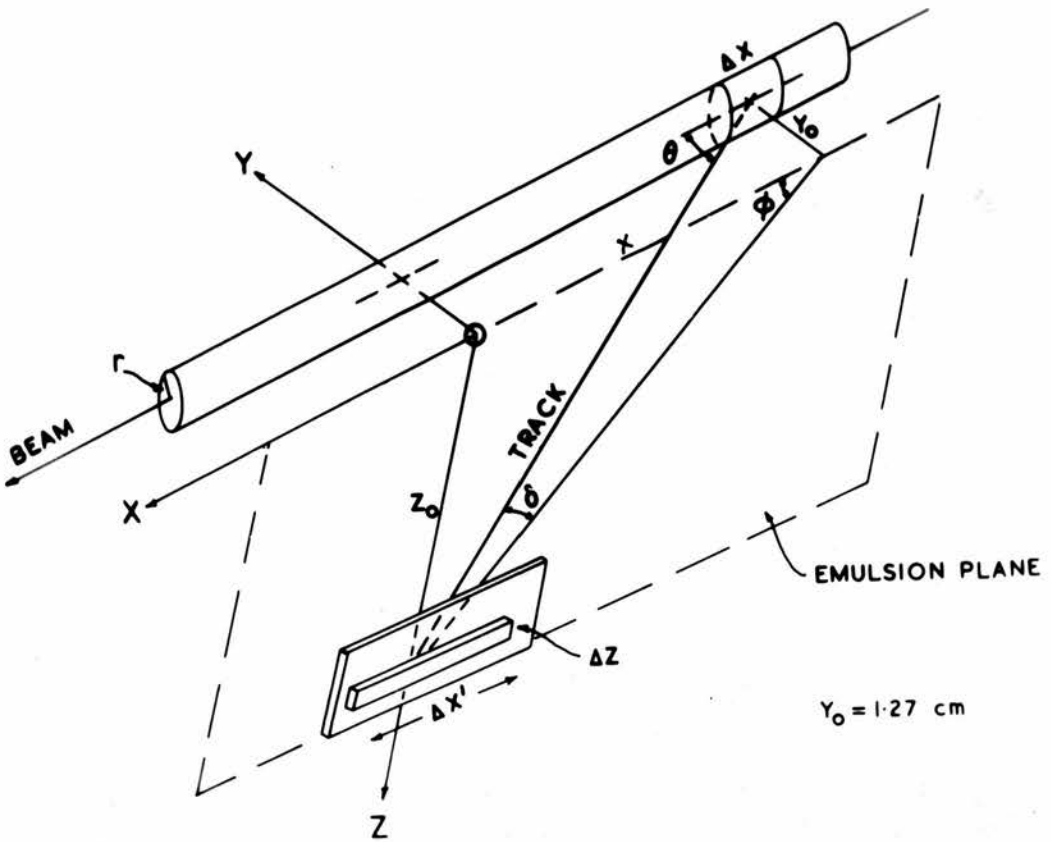
ΔX
θ
Y
Y₀
φ
X
BEAM
r
TRACK
X
Z₀
δ
EMULSION PLANE
ΔZ
ΔX'
Z
Y₀ = 1·27 cm

subtended by ΔA at the beam element is

$$\Delta\Omega = (\Delta A/R^2)\sin\delta = (\Delta A/x^2\sec^2\theta).(y_o/x\sec\theta)$$

In practice, $\Delta x'$ is made the length of strip scanned, but is still very small compared with the length of the irradiated column of gas in the camera; Δz is sufficiently small for z to be regarded as fixed at its average value z_o. Then θ will depend on x only, the relation being

$$x^2\tan^2\theta = y_o^2 + z_o^2$$

so that we may substitute $\Delta x = x\Delta\theta/\sin\theta\cos\theta$. Thus the number of tracks entering ΔA at angle θ to the beam is given in terms of θ by the expression

$$f(\theta)\Delta\theta = \pi r^2 N\nu\sigma(\theta)(\Delta A y_o/x^3\sec^3\theta).(x\Delta\theta/\sin\theta\cos\theta)$$

$$= \pi r^2 N\nu\sigma(\theta)\Delta A\left\{y_o/(y_o^2 + z_o^2)\right\}\sin\theta\Delta\theta$$

This result shows that the number of tracks counted at angle θ is proportional to $\sigma(\theta)\sin\theta$, and should be divided by $\sin\theta$ to yield the true angular distribution.

To enable the total cross section σ to be estimated by counting the total number F of tracks found <u>at all angles</u>, it is necessary to integrate $f(\theta)$ over $0 \leqslant \theta \leqslant 2\pi$; this will involve the integral

$$\int_0^{2\pi} \sigma(\theta)\sin\theta d\theta = (1/2\pi)\int_{4\pi} \sigma(\theta)d\Omega = \sigma/2\pi$$

Thus

$$F = \pi r^2 N \nu \Delta A \left\{ y_o / (y_o^2 + z_o^2) \right\} (\sigma / 2\pi)$$

or

$$\sigma = 2F(y_o^2 + z_o^2)/N\nu r^2 \Delta A y_o$$

Modifications of this basic theory have been made for the effects of beam polarization, finite beam cross section and finite scanned area, but in no case do these exceed 2%.

Typewritten by the Author